



1 **Memory effects on greenhouse gas emissions (CO₂, N₂O and CH₄) following 2 grassland restoration?**

3

4

5 Lutz Merbold^{1,2*}, Charlotte Decock³⁺, Werner Eugster¹, Kathrin Fuchs⁴, Benjamin Wolf⁴, Nina
6 Buchmann¹ and Lukas Hörtnagl¹

7

8 ¹ Department of Environmental Systems Science, Institute of Agricultural Sciences, Grassland
9 Sciences Group, ETH Zurich, Universitätsstrasse 2, 8092 Zürich, Switzerland

10 ² Mazingira Centre, International Livestock Research Institute (ILRI), Old Naivasha Road, PO
11 Box 30709, 00100 Nairobi, Kenya

12 ³ Department of Environmental Systems Science, Institute of Agricultural Sciences,
13 Sustainable Agro-ecosystem Group, ETH Zurich, Universitätsstrasse 2, 8092 Zürich,
14 Switzerland, ⁺ now at: Department of Natural Resources Management and Environmental
15 Sciences, California State University, San Luis Obispo, California, USA

16 ⁴ Institute for Meteorology and Climate Research (IMK-IFU), Karlsruhe Institute of
17 Technology (KIT), Kreuzeckbahnstrasse 19, 82467 Garmisch-Partenkirchen, Germany

18

19 * corresponding author: l.merbold@cgiar.org

20

21

22 **Keywords:** eddy covariance, global warming potential, manual static chamber, management,
23 background greenhouse gas emissions, ploughing, fertilization

24

25 **Abstract**

26 A five-year greenhouse gas (GHG) exchange study of the three major gas species (CO₂, CH₄
27 and N₂O) from an intensively managed permanent grassland in Switzerland is presented.
28 Measurements comprise two years (2010/2011) of manual static chamber measurements of
29 CH₄ and N₂O, five years of continuous eddy covariance (EC) measurements (CO₂/H₂O – 2010-
30 2014) and three years (2012-2014) of EC measurement of CH₄ and N₂O. Intensive grassland
31 management included both regular and sporadic management activities. Regular management
32 practices encompassed mowing (3-5 cuts per year) with subsequent organic fertilizer
33 amendments and occasional grazing whereas sporadic management activities comprised



34 grazing or similar activities. The primary objective of our measurements was to compare pre-
35 ploughing to post-ploughing GHG exchange and to identify potential memory effects of such
36 a substantial disturbance on GHG exchange and carbon (C) and nitrogen (N) budgets. In order
37 to include measurements carried with different observation techniques, we tested two different
38 measurement techniques jointly in 2013, namely the manual static chamber approach and the
39 eddy covariance technique, to quantify the GHG exchange from the observed grassland site.
40 Our results showed that there were no memory effects on N₂O and CH₄ emissions after
41 ploughing, whereas the CO₂ uptake of the site considerably increased when compared to post-
42 restoration years. In detail, we observed large losses of CO₂ and N₂O during the year of
43 restoration. In contrast, the grassland acted as a carbon sink under usual management, i.e. the
44 time periods (2010-2011 and 2013-2014). Enhanced emissions/emission peaks of N₂O (defined
45 as exceeding background emissions $< 0.21 \pm 0.55 \text{ nmol m}^{-2} \text{ s}^{-1}$ (SE = 0.02) for at least two
46 sequential days and the seven-day moving average exceeding background emissions) were
47 observed for almost seven continuous months after restoration as well as following organic
48 fertilizer applications during all years. Net ecosystem exchange of CO₂ (NEE_{CO₂}) showed a
49 common pattern of increased uptake of CO₂ in spring and reduced uptake in late fall. NEE_{CO₂}
50 dropped to zero and became positive after each harvest event. Methane (CH₄) exchange in
51 contrast to N₂O showed minor net uptake of methane seen by the static chambers and small net
52 release of methane seen by the eddy covariance method. Overall, CH₄ exchange was of
53 negligible importance for both, the GHG budget as well as for the carbon budget of the site.
54 Our results stress the inclusion of grassland restoration events when providing cumulative sums
55 of C sequestration and/or global warming potentials (GWPs). Consequently, this study further
56 highlights the need for continuous long-term GHG exchange observations as well as the
57 implementation of our findings into biogeochemical process models to track potential GHG
58 mitigation objectives as well as to predict future GHG emission scenarios reliably.

59
60
61
62
63
64
65
66
67



68 1 Introduction

69

70 Grassland ecosystems are commonly known for their provisioning of forage, either directly via
71 grazing of animals on site, or indirectly by regular biomass harvest and preparation of silage
72 or hay. Simultaneously, grasslands have further been acknowledged for their greenhouse gas
73 (GHG) mitigation and soil carbon sequestration potential (Lal, 2004; Smith et al., 2008).
74 However, greenhouse gas emissions from grasslands, particularly N₂O and CH₄ have been
75 shown to offset net carbon dioxide equivalent (CO₂-eq.) gains (Dengel et al., 2011; Hörtengl
76 et al., 2018; Hörtengl and Wohlfahrt, 2014; Merbold et al., 2014; Schulze et al., 2009). Still,
77 datasets containing continuous measurements of all three major GHGs (CO₂, CH₄ and N₂O) in
78 grassland ecosystems remain limited (Hörtengl et al., 2018), include a single GHG only, or
79 focus on specific management activities (Fuchs et al., 2018; Krol et al., 2016). At the same
80 time such datasets are extremely valuable by providing key training datasets for
81 biogeochemical process models (Fuchs et al., 2020).

82 Here we investigate the GHG exchange of the three major trace gases (CO₂, CH₄ and N₂O)
83 over five consecutive years in a typical managed grassland on the Swiss plateau. Our study
84 includes the application of traditional chamber measurements and state-of-the-art GHG
85 concentration measurements with a quantum cascade laser absorption spectrometer and a sonic
86 anemometer in an eddy covariance setup (Eugster and Merbold, 2015). Prior to our
87 measurements we hypothesized continuous (over several years) losses of CO₂, CH₄ and N₂O
88 following dramatic managements events such as ploughing occurring at irregular time intervals
89 with subsequent high emissions of N₂O in the following years after disturbance. We further
90 hypothesized an increased carbon uptake strength compared to the pre-ploughing years.
91 Methane emissions were hypothesized to be of minor importance due to the limited time of
92 grazing animals on site (Merbold et al., 2014).

93 Up to date the majority of greenhouse gas exchange research has focused on CO₂, with less
94 focus on the other two important GHGs N₂O and CH₄, even though an increased interest in
95 these other gas species has become visible in recent years (Ball et al., 1999; Cowan et al., 2016;
96 Krol et al., 2016; Kroon et al., 2007, 2010; Necpálová et al., 2013). The existing exceptions
97 are often referred to as “high-flux” ecosystems, namely wetlands and livestock production
98 system in terms of CH₄ (Balocchi et al., 2012; Felber et al., 2015; Laubach et al., 2016; Teh
99 et al., 2011) and agricultural ecosystems such as bioenergy system with considerable N₂O
100 emissions (Fuchs et al., 2018; Krol et al., 2016; Skiba et al., 1996, 2013; Zenone et al., 2016;



101 Zona et al., 2013). Agricultural ecosystems and specifically grazed systems are characterized
102 by GHG emissions caused through anthropogenic activities. These activities lead to changes
103 in GHG emission patterns and include harvests, amendments of fertilizer and/or pesticides and
104 less frequently occurring ploughing, harrowing and re-sowing events. While ploughing has
105 been shown to lead to considerable short-term emissions of CO₂ and N₂O (Buchen et al., 2017;
106 Hörtnagl et al., 2018; MacKenzie et al., 1997; Merbold et al., 2014; Vellinga et al., 2004),
107 regular harvests have been shown to lead to increased CO₂ uptake (Zeeman et al., 2010) and
108 grazing leads to large CH₄ emissions ((Dengel et al., 2011; Felber et al., 2015). Other studies
109 showed contrary results with reduced N₂O emissions following ploughing of a drained
110 grassland when compared to a fallow in Canada (MacDonald et al., 2011).
111 Still, the full range of management activities occurring in intensively managed grasslands and
112 their respective impact on GHG exchange has not been investigated in detail. In a recent
113 synthesis including grasslands located along an altitudinal gradient in Central Europe, Hörtnagl
114 et al. (2018) highlighted the most important abiotic drivers of CO₂ (light, water availability and
115 temperature), CH₄ (soil water content, temperature and grazing) and N₂O exchange (water
116 filled pore space and soil temperature). Similarly, the study elaborated the variation in
117 management intensity and subsequent variations in GHG exchange across sites, stressing the
118 need for more case studies based on continuous GHG observations to improve existing
119 knowledge and close remaining knowledge gaps (Hörtnagl et al., 2018). Besides natural
120 variation in environmental variables, irregularly occurring events (e.g. extreme events) such as
121 dry spells or extraordinary wet periods can further impact ecosystem GHG exchange (Chen et
122 al., 2016; Hartmann and Niklaus, 2012; Hopkins and Del Prado, 2007; Mudge et al., 2011;
123 Wolf et al., 2013). While drought has been shown to reduce CO₂ uptake in forests (Ciais et al.,
124 2005) whereas dry spells did not affect CO₂ uptake in grasslands (Wolf et al., 2013), flooding
125 leads primarily to enhanced CH₄ emissions (Knox et al., 2015) and large precipitation events
126 can lead to plumes of N₂O (Fuchs et al., 2018; Zona et al., 2013) similar to freeze-thaw events
127 (Butterbach-Bahl et al., 2011; Matzner and Borken, 2008) to name only some examples.
128 Consequently, understanding both, anthropogenic impacts such as management besides
129 environmental impacts on ecosystem GHG exchange, are crucially important to suggest
130 appropriate climate change mitigation as well as adaptations strategies for future land
131 management with ongoing climate change.
132 Different measurement techniques to quantify the net GHG exchange in ecosystems are known
133 and the most common approaches are either GHG chamber measurements or the eddy
134 covariance (EC) technique. Static manual chamber measurements have been used for more



135 than a century to quantify CO₂ emissions (Lundegardh, 1927) and their application has further
136 been expanded during the last decades to quantify losses of the three major GHGs, CO₂, N₂O
137 and CH₄ from soils, respectively (Imer et al., 2013; Pavelka et al., 2018a; Pumpanen et al.,
138 2004; Rochette et al., 1997). Even though more complex in technology and assumptions made
139 before carrying out measurements, the eddy covariance (EC) technique has become a valuable
140 tool to derive ecosystem integrated CO₂ and H₂O_{vapour} exchange across the globe (Baldocchi,
141 2014; Eugster and Merbold, 2015). The technique has been further extended to continuous
142 measurements of CH₄ and N₂O with the development of easy field-deployable fast-response
143 analyzers during the last decade (Brümmer et al., 2017; Felber et al., 2015; Kroon et al., 2007;
144 Nemitz et al., 2018a). Each of the two approaches has its strengths and weaknesses and it is
145 beyond the scope of this study to discuss each of them in detail. However, we refer to a set of
146 reference papers highlighting the advantages and disadvantages of each technique separately
147 (chambers: (Ambus et al., 1993; Brümmer et al., 2017; Pavelka et al., 2018a); eddy covariance:
148 (Baldocchi, 2014; Denmead, 2008; Eugster and Merbold, 2015; Nemitz et al., 2018a)).
149 The overall objective of this study was to investigate the net GHG exchange (CO₂, CH₄ and
150 N₂O) before and after grassland restoration and thus fill existing knowledge gaps caused by
151 limited amounts of GHG exchange data from intensively managed grasslands. The specific
152 goals were: (i) to assess pre- and post-ploughing GHG exchange in a permanent grassland in
153 central Switzerland; (ii) to briefly compare two different measurement techniques, namely
154 eddy covariance and static greenhouse gas flux chambers to quantify the GHG exchange in a
155 business-as-usual year; (iii) to identify changes in GHG exchange after multiple management
156 activities; and (iv) to provide a partial carbon (C) and nitrogen (N) budget of the site. Based on
157 our results we provide suggestions for future research approaches to further understand
158 ecosystem GHG exchange, to mitigate GHG emissions and to ensure nutrient retention at the
159 site for sustainable production from permanent grasslands in the future.

160
161
162
163
164
165
166
167



168 2 Material and Methods

169 2.1 Study site

170 The Chamau grassland site (Fluxnet identifier - CH-Cha) is located in the pre-alpine lowlands
171 of Switzerland at an altitude of 400 m a.s.l. (47°12' 37"N, 8°24'38"E) and characterized by
172 intensive management (Zeeman et al., 2010). The site is divided into two parcels (Parcel A and
173 B) with occasionally slightly different management regimes [see also Fuchs et al., 2018]. Mean
174 annual temperature (MAT) is 9.1 °C, and mean annual precipitation (MAP) is 1151 mm. The
175 soil type is a Cambisol with a pH ranging between 5 and 6, a bulk density between 0.9 and 1.3
176 kg m⁻³ and a carbon stock of 55.5–69.4 t C ha⁻¹ in the upper 20 cm of the soil. The common
177 species composition consists of Italian ryegrass (*Lolium multiflorum*) and white clover
178 (*Trifolium repens L.*). For more details of the site we refer to Zeeman et al., (2010).

179 CH-Cha is intensively managed, with activities being either recurrent – referred to as
180 usual/regular - or sporadic. Usual management refers to regular mowing and subsequent
181 organic fertilizer application in form of liquid slurry (up to 7 times per year). In addition, the
182 site is occasionally grazed by sheep and cattle for few days in early spring and/or fall (H.-R.
183 Wettstein personal communication, Table S1). Sporadic activities aim at maintaining the
184 typical fodder species composition and comprise reseeding, herbicide and pesticide application
185 or irregular ploughing and harrowing on an approximately decadal timescale (Merbold et al.,
186 2014). By such activity, mice are eradicated and a high-quality sward for fodder production is
187 re-established following weed contamination. Specific information on management activity
188 (timing, type of management, amount of biomass harvested) were reported by the farmers on
189 site (Table S1). Additionally, representative samples of organic fertilizer were collected shortly
190 before fertilizer application events and sent to a central laboratory for nutrient content analysis
191 (Labor fuer Boden- und Umweltanalytik, Eric Schweizer AG, Thun, Switzerland). Harvest
192 estimates were compared to estimates based on destructive sampling of randomly chosen plots
193 (n = 10) in the years 2010, 2011, 2013 and 2014. The amount of harvested biomass in the year
194 2012 was based on a calibration of the values presented by the farmer in comparison to the on-
195 site destructive harvests in previous and following years (Table S1).

196

197 2.2 Eddy covariance flux measurements

198 2.2.1 Eddy covariance setup

199 The specific site characteristics with two prevailing wind directions (North-northwest and
200 South-south east) allows continuous observations of both management parcels. It is



noteworthy, that the separation of the two parcels is done exactly at the location of the tower.
See Zeeman et al. (2010) and Fuchs et al. (2018) for further details. The eddy covariance setup consisted of a three-dimensional sonic anemometer (2.4 m height, Solent R3, Gill Instruments, Lymington, UK), an open-path infrared gas analyzer (IRGA, LI-7500, LiCor Biosciences, Lincoln, NE, USA) to measure the concentrations of CO₂ and H₂O_{vapour} and a recently developed continuous-wave quantum cascade laser absorption spectrometer (mini-QCLAS - CH₄, N₂O, H₂O configuration, Aerodyne Research Inc., Billerica, MA, USA) to measure the concentrations of CH₄, N₂O, and H₂O_{vapour}. 3D wind components (u, v, w), CO₂ and H₂O_{vapour} concentration data from the IRGA were collected at a 20 Hz time interval, whereas concentrations of CH₄ and N₂O were collected at a 10 Hz rate from the QCLAS. The QCLAS provided the dry mole fraction for both trace gases (CH₄ and N₂O), and data were transferred to the data acquisition system (MOXA embedded Linux computer, Moxa, Brea, CA, USA) via an RS-232 serial data link and merged with the sonic anemometer and IRGA data streams in near-real time (Eugster and Plüss, 2010). Important to note is that the QCLAS was stored in a temperature-controlled box (temperature variation during the course of a single day was reduced to < 2 K) and located approximately 4 meters away from the EC tower to avoid long tubing. Total tube length from the inlet near the sonic anemometer to the measurement cell was 6.5 m. The inlet consisted of a coarse sinter filter (common fuel filter used in model cars) and a fine vortex filter (mesh size 0.3 µm and a water trap) installed directly before the QCLAS. Filters were changed monthly or if the cell pressure in the laser dropped by more than 2 torr. Flow rate of approximately 15 l min⁻¹ was achieved with a large vacuum pump (BOC Edwards XDS-35i, USA and TriScoll 600, Varian Inc., USA – the latter was used during maintenance of the Edwards pump). The pumps were maintained annually and replaced twice due to malfunction during the observation period. The infrared gas analyzer was calibrated to known concentrations of CO₂ and H₂O each year. The QCLAS did not need calibration due to its operating principles, and an internal reference cell (mini-QCL manual, Aerodyne Research Inc., Billerica, MA, USA) eased finding the absorption spectra after each restart of the analyzer.

2.2.2 Eddy covariance flux processing, post-processing and quality control

Half-hourly raw fluxes of CO₂, CH₄, N₂O (F_{GHG} , µmol m⁻² s⁻¹) were calculated as the covariance between turbulent fluctuations of the vertical wind speed and the trace gas species mixing ratio, respectively (Baldocchi, 2003; Eugster and Merbold, 2015). Open-path infrared gas analyzer (IRGA) CO₂ measurements were corrected for water vapor transfer effects (Webb et al., 1980). A 2-dimensional coordinate rotation was performed to align the coordinate system



235 with the mean wind streamlines so that the vertical wind vector $\vec{w} = 0$. Turbulent departures
236 were calculated by Reynolds (block) averaging of 30 min data blocks. Frequency response
237 corrections were applied to raw fluxes, accounting for high-pass and low-pass filtering for the
238 CO₂ signal based on the open-path IRGA as well as for the closed-path CH₄ and N₂O data
239 (Fratini et al., 2014). All fluxes were calculated using the software *EddyPro* (version 6.0, LiCor
240 Biosciences, Lincoln, NE, USA) (Fratini and Mauder, 2014).

241 The quality of half-hourly raw time series was assessed before flux calculations following
242 (Vickers and Mahrt, 1997). Raw data were rejected if (a) spikes accounted for more than 1 %
243 of the time series, (b) more than 10 % of available data points were significantly different from
244 the overall trend in the 30 min time period, (c) raw data values were outside a plausible range
245 ($\pm 50 \mu\text{mol m}^{-2} \text{s}^{-1}$ for CO₂, $\pm 300 \text{ nmol m}^{-2} \text{s}^{-1}$ for N₂O and $\pm 1 \mu\text{mol m}^{-2} \text{s}^{-1}$ for CH₄) and (d)
246 window dirtiness of the IRGA sensor exceeded 80 %. Only raw data that passed all quality
247 tests were used for flux calculations. Half-hourly flux data were rejected if (e) fluxes were
248 outside a physically plausible range, (f) the steady state test exceeded 30 % and (g) the
249 developed turbulent conditions test exceeded 30 % (Foken et al., 2006).

250 Between 1st January 2010 and 31st December 2014 64572 (88% of all possible data) raw 30-
251 min flux values were calculated for CO₂, of which 42865 (57.8%) passed all quality tests and
252 were used for analyses in the present study (Table 1). The amount of available flux values for
253 N₂O and CH₄ were less, since we were only capable to continuously measure both gases from
254 2012 onwards (Table 1). Flux values in this manuscript are given as number of moles of
255 matter/mass of matter per ground surface area and unit time. Negative fluxes represent a flux
256 of a specific gas species from the atmosphere into the ecosystem, whereas positive fluxes
257 represent a net loss from the system.

258

259 **2.3 Static greenhouse gas flux chambers**

260 *2.3.1 Manual static GHG chamber setup*

261 Static manual opaque GHG chambers were installed within the footprint of the site to measure
262 soil fluxes in 2010 and 2011 (n = 16) as well as during summer 2013 (n = 10). The chambers
263 were made of polyvinyl chloride tubes with a diameter of 0.3 m (Imer et al., 2013). The average
264 headspace height was $0.136 \text{ m} \pm 0.015 \text{ m}$ and average insertion depth of the collars into the
265 soil was $0.08 \text{ m} \pm 0.05 \text{ m}$. During sampling days with vegetation larger than 0.3 m inside the
266 chamber, collar extensions (0.45 m) were used (2013 only). Chamber lids were equipped with
267 reflective aluminium foil to minimize heating inside the chamber during the period of actual
268 measurement. Spacing between the chambers was approximately seven m and an equal number



269 of chambers were installed in each parcel. For further details we refer to Imer et al. (2013).
270 Chamber measurements were carried out on a weekly basis during the growing season in all
271 three years (2010, 2011 and 2013), and at least once a month during the winter season in 2010
272 and 2011. More frequent measurements of N₂O emissions (every day) were performed
273 following fertilization events in 2013 for seven consecutive days after each event. Besides this,
274 an intensive measurement campaign lasting 48 hours (two-hour measurement interval) was
275 carried out in September 2010.

276

277 *2.3.2 GHG concentrations measurements*

278 During each chamber closure four gas samples were taken, one immediately after closure and
279 then in approximately ten-minute time increments. With this approach, we guaranteed that the
280 chambers were no longer closed than 40 minutes to avoid potential saturation effects. Syringes
281 (60 ml volume) were inserted into the chambers lid septa to take the gas samples. The collected
282 air sample was injected into pre-evacuated 12 ml vials (Labco Limited, Buckinghamshire, UK)
283 in the next step. Prior to the second, third and fourth sampling of each chamber, the air in
284 chamber headspace was circulated with the syringe volume of air from the chamber headspace
285 to minimize effects of built-up concentration gradients inside the chamber.

286 Gas samples were analyzed for their respective CO₂, CH₄ and N₂O concentrations in the lab as
287 soon as possible after sample collection and not stored for more than a few days. Gas sample
288 analysis was performed with a gas chromatograph (Agilent 6890 equipped with a flame
289 ionization detector, a methanizer - Agilent Technologies Inc., Santa Clara, USA - and an
290 electron capture detector – SRI Instruments Europe GmbH, 53604 Bad Honnef, Germany) as
291 described by Hartmann and Niklaus (2012).

292

293 *2.3.3 GHG chamber flux calculations and quality control*

294 GHG fluxes were calculated based on the rate of gas concentration change inside the chamber
295 headspace. Data processing, which included flux calculation and quality checks, was carried
296 out with the statistical software R (R Development Core Team, 2010). Thereby the rate of
297 change was calculated by the slope of the linear regression of gas concentration over time. Flux
298 calculation was based on the common equation containing GHG concentration (c in nmol mol⁻¹ for CH₄ and N₂O), time (t in seconds), atmospheric pressure (p in Pa), the headspace volume
300 (V in m⁻³), the universal gas constant (R = 8.3145 m⁻³ Pa K⁻¹ mol⁻¹), ambient air temperature
301 (Ta in K) and the surface area enclosed by the chamber (A in m²) (equation 1 in Imer et al.
302 (2013)).



303 Flux quality criteria were based on the fit of the linear regression. If the correlation coefficient
304 of the linear regression (r^2) was < 0.8 the actual flux value was rejected from the subsequent
305 data analysis. Furthermore, if the slope between the 1st and 2nd GHG concentration
306 measurement deviated considerably from the following concentrations we omitted the first
307 value and calculated the flux based on three instead of four samples. Mean chamber GHG
308 fluxes were then calculated as the arithmetic mean of all available individual chamber fluxes
309 for each date. A total of 60 GHG flux calculations (CH₄ and N₂O) were available for the years
310 2010 and 2011. Another 52 N₂O flux values were available for the five-month peak-growing
311 season in 2013.

312

313 *2.4 Gapfilling and annual sums of CO₂, CH₄, and N₂O*

314 Up to date a common strategy to fill gaps in EC data of CH₄ and N₂O has not been agreed on.
315 The commonly used methods are simple linear approaches (Mishurov and Kiely, 2011) or the
316 application of more sophisticated tools such as artificial neural networks (Dengel et al., 2011).
317 The difficulty of finding an adequate gap-filling strategy results from the fact that emission
318 pulses of either N₂O or CH₄ remain challenging to predict. Similarly, different measurement
319 approaches – i.e. low temporal resolution manual GHG chambers compared to high temporal
320 resolution eddy covariance measurements - need different gap-filling approaches (Mishurov
321 and Kiely, 2011; Nemitz et al., 2018). In order to keep the gap-filling methods as simple and
322 reliable as possible, we used a running median (30 and 60 days for eddy covariance based and
323 chamber based CH₄ and N₂O fluxes, respectively). A similar approach was recently chosen by
324 Hörtnagl et al. (2018) due to its sensitivity to peaks in the GHG exchange data.

325 In contrast to CH₄ and N₂O various well-established approaches to fill CO₂ flux data exist
326 (Moffat et al., 2007). Here, we filled gaps in CO₂ exchange data following the marginal
327 distribution sampling method (Reichstein et al., 2005) which was implemented in the R
328 package REddyProc (<https://r-forge.r-project.org/projects/reddyproc/>).

329 Calculation of the global warming potential (GWP) given in CO₂-equivalents followed the
330 recommendations given in the 5th Assessment Report of the Intergovernmental Panel on
331 Climate Change (IPCC), with CH₄ having a 34 and N₂O a 298 times greater GWP than CO₂
332 on a per mass basis over a time horizon of 100 years including climate-carbon feedbacks
333 (Stocker et al., 2013).

334

335 *2.5 Meteorological and phenological data*

336 Flux measurements were accompanied by standard meteorological measurements. These



337 included observations of soil temperature (depths of 0.01, 0.02, 0.05, 0.10, and 0.15 m, TL107
338 sensors, Markasub AG, Olten, Switzerland), soil moisture (depths of 0.02 and 0.15 m, ML2x
339 sensors, Delta-T Devices Ltd., Cambridge, UK) and air temperature (2 m height, Hydroclip S3
340 sensor, Rotronic AG, Switzerland). Furthermore, we measured the radiation balance including
341 short-wave incoming and outgoing radiation, long-wave incoming and outgoing radiation
342 (CNR1 sensor with ventilated Markasub housing, Kipp and Zonen, Delft, the Netherlands) as
343 well as photosynthetically active radiation at 2 m height (PARlite sensor, Kipp and Zonen,
344 Delft, the Netherlands). All data were stored as 30 min averages on a datalogger in a climate-
345 controlled box on site (CR10X, Campbell Scientific, Logan, UT, USA).

346

347

348

349

350

351

352

353

354

355

356

357

358

359

360

361

362

363

364

365

366

367

368

369



370 **3 Results**

371 *3.1 General site conditions*

372 The Chamau study site (CH-Cha) experienced meteorological conditions typical for the site
373 during the five-year observation period. Summer precipitation commonly exceeded winter
374 precipitation (Figure 1a). A spring drought was recorded from March till May 2011 (Wolf et
375 al., 2013), leading to considerably lower soil water content than in previous and following years
376 (Figure 1a). Average daily air temperatures rose up to 26.7 °C (27th July 2013) during summer
377 and average daily temperature in winter dropped as low as -12.7 °C (6th February 2012, Figure
378 1b) with soil temperature following in a dampened pattern (Figure 1b). Average daily
379 photosynthetic photon flux density did not differ considerably over the five-year observation
380 period (Figure 1c). The site rarely experienced snow cover during winter (Figure 1b).

381 The complexity in management activities becomes apparent when comparing business as usual
382 years (e.g. 2011) with the restoration year (2012, Figure 2a and b), highlighting the importance
383 of grassland restoration to maintain productivity yields. Prior to 2012 an obvious decline in
384 productivity with larger C and N inputs was found compared to the outputs in the years after
385 restoration (2013 and 2014, Figure 2a and b).

386

387 *3.2 EC N₂O fluxes vs. chamber derived N₂O fluxes*

388 In 2013, we had the chance of comparing N₂O fluxes measured with two considerably different
389 GHG measurement techniques, namely eddy covariance and static chambers. The chambers
390 (n=10) were installed within the EC footprint. Our results reveal a similar temporal pattern,
391 with increased N₂O losses being captured by both methodologies following fertilizer
392 application. However, we could not identify a consistent bias of either technique (Figure 3a).
393 Direct comparison of both measurements revealed a reasonable correlation (slope m = 0.61, r²
394 = 0.4) and larger variation between both techniques with increasing flux values (Figure 3b).

395

396 *3.3 Temporal variation of GHG exchange*

397 Fluxes of CO₂ and N₂O showed considerable variation between and within years. This variation
398 primarily occurs due to management activities and seasonal changes in meteorological
399 variables (Figures 1 and 4). In contrast, methane fluxes did not show a distinct seasonal pattern.

400

401

402



403 *CO₂ exchange*

404 In pre-ploughing years (2010 and 2011), the Chamau site showed 60 % lower CO₂ uptake
405 compared to the post-ploughing years (2013 and 2014, Table 2). All four non-ploughing years
406 revealed largest CO₂ uptake rates in late spring (daily averaged peak uptake rates were >10
407 µmol CO₂ m⁻² s⁻¹, March and April, Figure 4a). Besides the seasonal effects a clear impact of
408 harvest events could be identified, with abrupt changes from net uptake of CO₂ to either
409 reduced uptake or net loss of CO₂ (light blue arrows indicate harvest event, Figure 4a). A
410 similar but less pronounced effect was found following grazing periods (light and dark brown
411 arrow, Figure 4a). A complete switch from net uptake to net CO₂ release was observed during
412 the first three months of 2012, after ploughing and during re-cultivation of the grassland. In
413 this specific year, the site only experienced snow cover for few days (Figure 1c), temperatures
414 below 5 °C occurred more regularly than in all other years (Figure 1 b). Seasonal CO₂ exchange
415 was characterized by net release of CO₂ in winter (DJF), highest CO₂ uptake rates were
416 observed in spring (MAM), constant uptake rates during summer (JJA) which however were
417 lower than those measured in spring, and very low net release of CO₂ in fall (Table 3). Average
418 winter CO₂ exchange for the five-year observation period (gap-filled 30 min data) was 0.28 ±
419 5.68 µmol CO₂ m⁻² s⁻¹ (SE = 0.04, Table 3). The restoration year 2012 showed a slightly
420 different pattern with relatively large CO₂ release in winter and spring and considerably lower
421 uptake rates in summer. The years before the restoration (2010 and 2011) were characterized
422 by smaller net uptake rates during spring and summer when compared to the post-ploughing
423 years (2013 and 2014). Additionally, winter fluxes in 2010 and 2011 were positive (net release
424 of CO₂), while winter fluxes in the years 2013 and 2014 were showing a small but consistent
425 net uptake of CO₂ (Figure 4a, Table 3).

426

427 *CH₄ exchange*

428 While the individual static chamber measurements showed a very small but persistent net
429 uptake of methane, eddy covariance measurements were more than an order of magnitude
430 larger without revealing uptake or release (Figure 4b, different y axis). Overall, methane fluxes
431 were very low at both, the plot (chamber) and ecosystem scale (eddy covariance). Any peaks
432 expected due to freezing and thawing in late winter and early spring could not be found. Also,
433 commonly reported net emissions of methane during grazing were not seen (Figure 4b).
434 Seasonal differences of methane exchange did not show a clear pattern (Table 3).

435

436



437 *N₂O exchange*

438 N₂O exchange was low during most of the days over the five-year observation period,
439 fluctuating around zero (Figure 4c). However, clear peaks in N₂O emissions were observed
440 following fertilization events or periods with high rainfall after a dry period in summer (i.e.
441 summer 2013 and 2014, Figures 3a and 4c). While event driven N₂O emissions were commonly
442 on the order of 4 to 8 nmol N₂O m⁻² s⁻¹ (Figure 4c), N₂O emissions following ploughing and
443 subsequent re-sowing of the grassland in 2012 lead to up to three times as high N₂O emissions
444 (Figure 4c, year 2012, see also Merbold et al. (2014)). Similar to methane, enhanced N₂O
445 emissions in late winter or early spring as reported by other studies could not be identified
446 (Figure 4c).

447 Background fluxes were estimated by analysing all high temporal resolution flux data but
448 excluding the restoration year 2012 and all values one week after a management event. Daily
449 average background fluxes were 0.21 ± 0.55 nmol m⁻² s⁻¹ (SE = 0.02). Differences in N₂O
450 exchange over the course of individual years became obvious when splitting the dataset into
451 the four seasons (winter – DJF, spring – MAM, summer – JJA and fall – SON). In contrast to
452 CO₂ exchange that showed large net uptake rates in spring, N₂O emissions were largest during
453 summer (JJA) and lowest in winter (DJF). As highlighted for the other gases, the year of
454 grassland restoration showed a completely different picture (Table 3).

455

456 *3.4 Annual sums and Global Warming Potential (GWP) of CO₂, CH₄ and N₂O*

457 Annual sums showed a net uptake of CO₂ during the two pre-ploughing years
458 (-695 g CO₂ m⁻² yr⁻¹ and -978 g CO₂ m⁻² yr⁻¹ in 2010 and 2011 respectively). Up to three times
459 of this net uptake was reached in 2013 and 2014, the two post-ploughing years (-2046 g CO₂
460 m⁻² yr⁻¹ and -2751 g CO₂ m⁻² yr⁻¹, Table 2). In contrast, the ploughing year 2011 was
461 characterized by a net release of CO₂ (1447 g CO₂ m⁻² yr⁻¹).

462 The annual methane budget ranged from a negligible uptake in 2010 and 2011 (< 0.1 g CH₄ m⁻
463 ² yr⁻¹) to a minor release between 2012 and 2014 (26.8 – 55.2 g CH₄ m⁻² yr⁻¹).

464 The Chamau site was characterized by a net release of nitrous oxide over the five-year study
465 period. While N₂O emission ranged between 0.34 and 1.17 g N₂O m⁻² yr⁻¹ in the non-ploughing
466 years, the site emitted 4.36 g N₂O m⁻² yr⁻¹ in 2012.

467 The global warming potential (GWP), expressed as the yearly cumulative sum of all gases after
468 their conversion to CO₂-equivalents, was negative during all years (between -387 and -2577
469 CO₂-eq. m⁻²) except for the ploughing year 2012 (+2629 CO₂-eq. m⁻²).



470 Overall, CO₂ exchange contributed more than 90% to the total GHG balance in 2011, 2013 and
471 2014. Clearly, CH₄ exchange were of minimal importance for the GHG budget (Table 2). In
472 2010, the contribution of CO₂ to the site's GHG budget was almost 70%, and N₂O contributed
473 about 30%. Only in 2012, the year of restoration, CO₂ and N₂O exchange contributed almost
474 equally to the site's overall GHG budget (55.1% and 43.9%, respectively).

475

476 *3.5. Carbon and nitrogen budgets of the Chamau site between 2010 and 2014*

477 The Chamau site assimilated on average -441 ± 260 g CO₂-C m⁻² yr⁻¹ (4410 kg C ha⁻¹ yr⁻¹)
478 during the “business as usual” years (2010 and 2011 as well as 2013 and 2014). During the
479 restoration year the site lost 395 g CO₂-C m⁻² (3950 kg C ha⁻¹) (Table 2). Carbon losses (and/or
480 gains) from methane were < 1 g CH₄-C m⁻² during all five years. Losses of nitrogen ranged
481 from 0.2 g N₂O-N m⁻² (2 kg N ha⁻¹) in the non-ploughing years to 2.7 g N₂O-N m⁻² (27 kg N
482 ha⁻¹) in 2012 (Table 2).

483 Carbon and partial nitrogen budgets showed net gains in both parcels during the pre-ploughing
484 years (Table 4). Considerable net losses of carbon were calculated for the ploughing year, while
485 the same year was characterized by a net input of nitrogen. In contrast, the post-ploughing years
486 were again recognized as years with large net gains in carbon while at the same time showing
487 net losses of nitrogen. Over the observation period of 5 years, the Chamau grassland gained
488 approximately 4 t C ha⁻¹, excluding losses via leaching and deposition of C in form of dust.
489 During the same time, the site was characterized by a net input of approx. 70 kg N ha⁻¹.
490 However, the nitrogen budget did not consider losses in form of ammonia emissions (NH₃),
491 other reactive nitrogen gases (NO_x), deposition of N and leaching of N in form of NO₃⁻ and
492 NH₄⁺ (Table 4).

493

494

495

496

497

498

499

500

501

502



503 **4 Discussion**

504 The five-year measurement period is representative for other similarly managed grassland
505 ecosystems in Switzerland. Climate conditions were similar to the long-term average as
506 described in Wolf et al. (2013). Management activities, such as harvests and subsequent
507 fertilizer applications, were driven by overall weather conditions, (i.e. 2013 late spring, Figure
508 2a and b).

509

510 *4.1 Technical and methodological aspects*

511 Different techniques are currently applied to measure GHG fluxes from a variety of ecosystems
512 (Denmead, 2008), each having its advantages and disadvantages or being chosen for a specific
513 purpose or reason. A common approach to study individual processes or time periods
514 contributing to specific greenhouse gas emissions is to measure with GHG chambers on the
515 plot scale (Pavelka et al., 2018). Chamber methods have been widely used to derive annual
516 GHG and nutrient budgets (Barton et al., 2015; Butterbach-Bahl et al., 2013). Critical
517 assessments of the suitability and associated uncertainty in chamber derived GHG budgets in
518 relation to sampling frequency have been published by Barton et al. (2013). Existing studies
519 have not only compared the two measurement techniques employed in this study (manual
520 chambers and eddy covariance) in grasslands before, but also estimated annual emissions based
521 on differing methodologies (Flechard et al., 2007; Jones et al., 2017). Additional confidence in
522 our approach was obtained from the N₂O emissions during the summer period 2013, where
523 both measurement techniques ran in parallel (Figure 3a and b). Annual budgets derived by
524 applying similar gap-filling approaches to the individual datasets led to comparable results
525 (Table 2).

526 Our study found opposing net fluxes of methane when comparing chamber fluxes (2010 and
527 2011) with eddy covariance methane fluxes. Published studies carried out to investigate
528 grassland methane emissions with chambers mostly show a net uptake of methane (Beyer et
529 al., 2015; Chiavegato et al., 2015; Kim and Tanaka, 2015; Wei et al., 2015), while eddy
530 covariance based studies often show a net release of methane (Balocchi et al., 2012; Dengel
531 et al., 2011; Hörtnagl et al., 2018; Kroon et al., 2010). We identified three primary reasons for
532 this discrepancy: (1) the difference in spatial scales that the individual methods investigate; (2)
533 the different accuracy of both methods in detecting small fluxes; and (3) the system in which
534 researchers intend to investigate. In more detail: (1) a GHG chamber commonly covers only a
535 small area of the grassland (few cm² to m²) and unless the chamber is directly placed on a heap



536 of manure recently deposited by an animal, net methane fluxes are expected to show a small
537 uptake. Such small fluxes were observed on the Chamau site. We calculated detection limits
538 for the individual GHGs from our manual chambers following (Parkin et al., 2012). Detection
539 limits were $0.34 \pm 0.26 \text{ nmol m}^{-2} \text{ s}^{-1}$, $0.05 \pm 0.02 \text{ nmol m}^{-2} \text{ s}^{-1}$, and $0.06 \pm 0.06 \mu\text{mol m}^{-2} \text{ s}^{-1}$ for
540 CH₄, N₂O and CO₂, respectively, clearly indicating that methane fluxes measured by GHG
541 chambers in 2010/2011 were on average ($-0.16 \pm 0.16 \text{ nmol CH}_4 \text{ m}^{-2} \text{ s}^{-1}$, see Table 2) and thus
542 below the actual detection limit. The eddy covariance tower on the other hand has a much
543 larger area it “sees”. Measurements may include CH₄ emissions from ruminants when grazing
544 within the flux footprint area, and nearby stored manure, if the location is still within the flux
545 footprint area. However, we did not identify distinct methane peaks during occurrence of
546 grazing since grazing pressure was very low (Figure 2, Table S2). Consequently, methane
547 fluxes measured with EC fluctuating around zero (Figure 4b). Furthermore, considering the
548 assumptions made when calculating eddy covariance GHG fluxes as well as the precision of
549 the QCLAS used in this study for measuring CH₄ (approx. $1.5 \text{ nmol mol}^{-1}$ at 10 Hz), CH₄ flux
550 measurements at the CH-CHA site primarily consisted of noise measurements. N₂O fluxes in
551 contrast were much better constrained by both methods due to clear N₂O sources (i.e. fertilizer
552 amendments) and better sensitivity of the instruments used by both techniques for N₂O as
553 compared to CH₄.

554 As a third argument on why the sign of the flux differs between studies that used conventional
555 GHG chambers and eddy covariance towers is the researcher and the aim of the research project
556 itself. For instance, if the aim of a project is to study the spatial heterogeneity of GHG emissions
557 within a field a researcher may choose GHG chambers over the eddy covariance approach.
558 Annual budgets of a whole field on the other hand may be better derived with EC measurements
559 due to the continuity of the measurements (Eugster and Merbold, 2015). Besides the aim of a
560 research project, current GHG research primarily tends to quantify GHG exchange from
561 relevant sources, i.e. grazing cattle in the field, which can only be achieved by the EC approach
562 (or with invasive methods such as SF₆ as a tracer used in ruminant research) but not with
563 manual GHG chambers as done in existing studies that investigate GHG exchange from
564 pastures (Dengel et al., 2011).

565

566 *4.2 Annual GHG and nutrient budgets*

567 Net carbon losses and gains estimated for the CH-Cha site are in general within the range of
568 values estimated by Zeeman et al., (2010) for the years 2006 and 2007. The slightly higher
569 losses observed prior to ploughing may result from reduced productivity of the sward. This



570 becomes particularly visible when compared to the net ecosystem exchange (NEE) of CO₂
571 values for the years after restoration. Losses via leaching have previously been estimated to be
572 of minor importance at this site (Zeeman et al., 2010) and were therefore not considered in this
573 study. Considerably higher C gains during post-ploughing years were caused by enhanced plant
574 growth in spring and summer. Restoration is primarily done to eradicate weeds and rodents,
575 favouring biomass productivity of the fodder grass composition. Other grasslands in Central
576 Europe, i.e. sites in Austria, France and Germany, showed similar values for net ecosystem
577 exchange. Still, total C budgets as presented here are subject to considerable uncertainty which
578 is strongly depending on assumptions made for gap-filling etc. (Foken et al., 2004).
579 Nevertheless, the values reported here show the overall trend on C uptake/release of the site
580 and clearly exceed the uncertainty of ± 50 g C per year for eddy covariance studies as suggested
581 by (Baldocchi, 2003).

582 Methane was of negligible importance for the C budget of this site. This is primarily due to the
583 low grazing pressure at CH-Cha. Studies carried out on pastures in Scotland, Mongolia, France
584 and Western Switzerland have shown that grazing can largely contribute to ecosystem-scale
585 methane fluxes, in particular if ruminants such as cattle are populating the EC footprint (Dengel
586 et al., 2011; Felber et al., 2015; Schönbach et al., 2012). On the other hand, methane fluxes
587 from a pasture located in Austria at higher elevation showed small methane release and
588 moderate methane uptake, which was an order of magnitude higher than the minimal methane
589 uptake observed in our study by greenhouse gas chamber measurements during the years 2010
590 and 2011 (Hörtnagl and Wohlfahrt, 2014). The nitrous oxide budget reported for the years
591 without ploughing in this study coincides with values reported for other grasslands in Europe,
592 ranging from moist to dry climates and lower to higher elevations in Austria and Switzerland
593 (Hörtnagl et al., 2018; Imer et al., 2013; Skiba et al., 2013).

594
595 Nitrogen budgets varied largely between the years before and after ploughing. While the site
596 was characterized by large N amendments prior to ploughing and with reduced harvest, the
597 picture was completely the opposite during the years after ploughing, with considerably less N
598 inputs compared to the nitrogen removed from the field with the harvests. Farmers aim every
599 year at having a balanced N budget (fertilizer inputs = nutrients removed from the field).
600 Pasture degradation is the main motivation for enhanced fertilizer inputs in order to stabilize
601 forage productivity. Therefore, regular restoration of permanent pastures is absolutely
602 necessary (Cowan et al., 2016). So far, we identified only a single study that investigated the
603 net effects on GHG exchange following grassland restoration (Drewer et al., 2017).



604 5 Conclusion

605 This study in combination with an overview of available datasets on grassland restoration and
606 their consequences on GHG budgets highlights the overall need of additional observational
607 data. While restoration changed the previous C sink to a C source at the Chamau site, the wider
608 implication in terms of the GWP of the site when including other GHGs have long-term
609 consequences (i.e. in mitigation assessments). Furthermore, this study showed the large
610 variations in N inputs and N outputs from this grassland and the difficulty farmers face when
611 aiming for balanced N budgets in the field. Still, the current study focused on GHGs only and
612 can only partially constrain the N budget. Losses in form of NH₃, N₂ and NO_x need to be
613 quantified to fully assess N budgets besides the overall fact that GHG data following grassland
614 restoration remain largely limited to investigate long-term consequences.

615 Fortunately, these are likely to become available in the near future by the establishment of
616 environmental research infrastructures (i.e. ICOS in Europe, NEON in the USA or TERN in
617 Australia) that aim at standardized, high quality and high temporal resolution trace gas
618 observation of major ecosystems, including permanent grasslands. With these additional data,
619 another major constraint of producing defensible GHG and nutrient budgets, namely gap-filling
620 procedures, will likely be overcome. New and existing data can be used to derive reliable
621 functional relations and artificial neural networks (ANNs) at field to ecosystem scale that are
622 capable of reproducing in-situ measured data. Once this step is achieved, both the available
623 data as well the functional relations can be used to improve, to train and to validate existing
624 biogeochemical process models. Subsequently, reliable projections on both nutrient and GHG
625 budgets at the ecosystem scale that are driven by anthropogenic management as well as climatic
626 variability become reality.

627 The study stresses the necessity of including management activities occurring at low frequency
628 such as ploughing in GHG and nutrient budget estimates. Only then, the effect of potential
629 best-bet climate change mitigation options can be thoroughly quantified. The next steps in
630 GHG observations from grassland must not only focus on observing business as usual
631 activities, but also aim at testing the just mentioned best-bet mitigation options jointly in the
632 field while simultaneously in combination with existing biogeochemical process models.

633

634

635

636



637 6 Tables and Figures

638

639 **Table 1:** Data availability of GHG fluxes measured over the five-year observation period.
640 Values are given as all data possible, raw processed values and high quality (HQ) data, which
641 were then used in the analysis. High quality data are data with a quality flag "0" and "1" from
642 the EddyPro output only. Grey shaded areas represent time period where both methods (EC
643 and static chambers) were used simultaneously to estimate F_{N2O} .
644

645 **Table 2:** Annual average CO₂, CH₄ and N₂O fluxes and annual sums for the three GHGs as
646 well as carbon and nitrogen gains/losses per gas species. GWP were calculated for a 100-year
647 time horizon and based on the most recent numbers provided by IPCC (2013). Annual budgets
648 were derived from either gap-filled manual chamber (MC) or eddy covariance (EC)
649 measurements.
650

651 **Table 3:** Average GHG flux rates per season: winter (DJF), spring (MAM), summer (JJA) and
652 fall (SON). Values are based on gap-filled data to avoid bias from missing nighttime data
653 (predominantly relevant for CO₂). Data are only presented when continuous measurements
654 (eddy covariance data) were available.
655

656 **Table 4:** Carbon and partial nitrogen budgets (excluding NH₃, NO_x and N₂ emissions as well
657 as N deposition is not included) for the Chamau (CH-Cha) site in 2010- 2014. Values are given
658 in kg ha⁻¹. Inputs/gains are indicated with "-" and losses/exports are indicated with "+". While
659 management information was available for both parcels (A and B), flux measurements are an
660 integrate of both parcels.
661

662 **Table 5:** Existing studies investigating the GHG exchange over pastures following ploughing.
663 Results presented show the flux magnitude following ploughing and are rounded values of the
664 individual presented in the papers. Values were converted to similar units (mg CO₂-C m⁻² h⁻¹,
665 µg CH₄-C m⁻² h⁻¹ and µg N₂O-N m⁻² h⁻¹). Based on Web of Knowledge search July 15th 2017
666 with the search terms "grassland", "pasture", "greenhouse gas", "ploughing" and/or "tillage".
667 Only two studies representing conversion from pasture to cropland or other systems were
668 included in this table.
669

670 **Table S1:** Detailed management information for the two parcels under investigation at the
671 Chamau research station. Data are based on fieldbooks provided by the farm personnel as well
672 as in-situ measurements. Organic fertilizer samples were sent to a central laboratory for nutrient
673 content analysis (Labor fuer Boden- und Umweltanalytik, Eric Schweizer AG, Thun,
674 Switzerland). Destructive harvests ($n = 10$) of biomass were carried out in the years 2010, 2011,
675 2013 and 2014. Harvest estimates are based on values derived from the in-situ measurements
676 and data provided by the farm personnel. Detailed information on the grazing regime was
677 furthermore provided by the farm personnel in hand-written form (not shown).
678

679 **Figure 1:** Weather conditions during the years 2010 – 2014. Weather data were measured with
680 our meteorological sensors installed on site. (a) Daily sum of precipitation (mm) and soil water
681 content (SWC, blue line, m³ m⁻³) measured at 5 cm soil depth; (b) daily averaged air
682 temperature (°C), daily averaged soil temperature (grey line, °C) and days with snow cover
683 (horizontal bars); (c) daily averaged photosynthetic photon flux density (PPFD, µmol m⁻² s⁻¹).
684



684 Days with snow cover were identified with albedo calculations. Days with albedo > 0.45 were
685 identified as days with either snow or hoarfrost cover.

686

687 **Figure 2:** Management activities for both parcels (A and B in panels (a) and (b), respectively)
688 on the CH-Cha site. Overall management varied particularly in 2010 between both parcels,
689 whereas similar management took place between 2011 and 2014. Arrow direction indicates
690 whether carbon (C in kg ha⁻¹) and/or nitrogen (N in kg ha⁻¹) were amended to, or exported from
691 the site ("F_o" and "F_{o*}" - organic fertilizers, slurry/manure (red); "F_m" - mineral fertilizer (light
692 orange); "H" - harvest (light blue); "G_s" and "G_c" - grazing with sheep/cows (light/dark
693 brown). Other colored arrows visualize any other management activities such as pesticide
694 application ("P_h" - herbicide (light pink); "P_m" - molluscicide (dark pink); "T" - tillage (black),
695 "R" - rolling (light grey) and "S" - sowing (dark grey) which occurred predominantly in 2010
696 (parcel B) and 2012 (parcels A and B). Carbon imports and exports are indicated by black and
697 grey bars. Thereby black indicated the start of the specific management activities and grey the
698 duration (e.g. during grazing, "G_s"). Green colors indicate nitrogen amendments or losses, with
699 dark green visualizing the start of the activity and light green colors indicating the duration.
700 Sign convention: positive values denote export/release, negative values import/uptake.

701

702 **Figure 3:** (a) Temporal dynamics of N₂O fluxes measured with the eddy covariance (white
703 circles) and manual greenhouse gas chambers (black circles measured in 2013) – grey lines
704 indicate standard deviation. Arrows indicate management events ("H" = harvest, "F_o" =
705 organic fertilizer application (slurry), "P_h" = pesticide (herbicide) application). (b) 1:1
706 comparison between chamber based and eddy covariance based N₂O fluxes in 2013. The
707 dashed line represents the 1:1 line. ($y = mx + c$, $r^2 = 0.4$, $m = 0.61$, $c = 0.17$, $p < 0.0001$). Sign
708 convention: positive values denote export/release, negative values import/uptake.

709

710 **Figure 4:** Temporal dynamics of gap-filled daily averaged greenhouse gas (GHG) fluxes
711 (white circles): a) CO₂ exchange in $\mu\text{mol m}^{-2} \text{s}^{-1}$; (b) CH₄ exchange in $\text{nmol m}^{-2} \text{s}^{-1}$ and (c)
712 N₂O exchange in $\text{nmol m}^{-2} \text{s}^{-1}$. Coloured circles indicate manual chamber measurements. While
713 both GHGs, CH₄ and N₂O were measured in 2010 and 2011 (blue circles), N₂O only was
714 measured in 2013 (light blue circles). The grey dashed lines indicate the beginning of a new
715 year. Same color coding as used in Figure 3 a was used to highlight management activities.
716 Sign convention: positive values denote export/release, negative values import/uptake. Grey
717 lines behind the circles indicate standard deviation.

718

719

720

721

722

723

724

725

726

727

728



729

730

731

732

733 **7 Acknowledgements**

734 Funding for this study is gratefully acknowledged and was provided by the following projects:
735 Models4Pastures (FACCE-JPI project, SNSF funded contract: 40FA40_154245 / 1), GHG-
736 Europe (FP7, EU contract No. 244122), COST-ES0804 ABBA and SNF-R'EQUIP
737 (206021_133763). We are specifically thankful to Hans-Rudolf Wettstein, Ivo Widmer and
738 Tina Stiefel for providing crucial management data and support in the field. Further, this project
739 could not have been accomplished without the help from the technical team, specifically Peter
740 Plüss, Thomas Baur, Florian Käslin, Philip Meier and Patrick Flütsch. We greatly acknowledge
741 their help during the planning stage, and the endurance during the setup of the new QCLAS
742 system as well as regular trouble shooting of the Swissfluxnet Chamau (CH-Cha) research site.

743

744

745

746

747

748

749

750

751

752

753

754

755

756

757

758

759

760

761



762

763

764

765

766 8 References

767

768 Ambus, P., Clayton, H., Arah, J. R. M., Smith, K. A. and Christensen, S.: Similar N₂O flux
769 from soil measured with different chamber techniques, *Atmos. Environ. Part A, Gen. Top.*,
770 doi:10.1016/0960-1686(93)90078-D, 1993.

771

772 Baldocchi, D. D.: Assessing the eddy covariance technique for evaluating carbon dioxide
773 exchange rates of ecosystems: Past, present and future, *Glob. Chang. Biol.*, doi:10.1046/j.1365-
774 2486.2003.00629.x, 2003.

775

776 Baldocchi, D., Detto, M., Sonnentag, O., Verfaillie, J., Teh, Y. A., Silver, W. and Kelly, N.
777 M.: The challenges of measuring methane fluxes and concentrations over a peatland pasture,
778 *Agric. For. Meteorol.*, doi:10.1016/j.agrformet.2011.04.013, 2012.

779

780 Baldocchi, D.: Measuring fluxes of trace gases and energy between ecosystems and the
781 atmosphere - the state and future of the eddy covariance method, *Glob. Chang. Biol.*,
782 doi:10.1111/gcb.12649, 2014.

783

784 Ball, B. C., Scott, A. and Parker, J. P.: Field N₂O, CO₂ and CH₄ fluxes in relation to tillage,
785 compaction and soil quality in Scotland, *Soil Tillage Res.*, doi:10.1016/S0167-1987(99)00074-
786 4, 1999.

787

788 Barton, L., Wolf, B., Rowlings, D., Scheer, C., Kiese, R., Grace, P., Stefanova, K. and
789 Butterbach-Bahl, K.: Sampling frequency affects estimates of annual nitrous oxide fluxes, *Sci.
790 Rep.*, doi:10.1038/srep15912, 2015.

791

792 Beyer, C., Liebersbach, H. and Höper, H.: Multiyear greenhouse gas flux measurements on a
793 temperate fen soil used for cropland or grassland, *J. Plant Nutr. Soil Sci.*,
794 doi:10.1002/jpln.201300396, 2015.

795

796 Brümmer, C., Lyshede, B., Lempio, D., Delorme, J. P., Rüffer, J. J., Fuß, R., Moffat, A. M.,
797 Hurkuck, M., Ibrom, A., Ambus, P., Flessa, H. and Kutsch, W. L.: Gas chromatography vs.
798 quantum cascade laser-based N₂O flux measurements using a novel chamber design,
799 *Biogeosciences*, doi:10.5194/bg-14-1365-2017, 2017.

800

801 Buchen, C., Well, R., Helfrich, M., Fuß, R., Kayser, M., Gensior, A., Benke, M. and Flessa,
802 H.: Soil mineral N dynamics and N₂O emissions following grassland renewal, *Agric. Ecosyst.
803 Environ.*, doi:10.1016/j.agee.2017.06.013, 2017.

804

805 Butterbach-Bahl, K., Kiese, R. and Liu, C.: Measurements of biosphere atmosphere exchange
806 of CH₄ in terrestrial ecosystems, in *Methods in Enzymology.*, 2011.

807



- 808 Butterbach-Bahl, K., Baggs, E. M., Dannenmann, M., Kiese, R. and Zechmeister-Boltenstern,
809 S.: Nitrous oxide emissions from soils: How well do we understand the processes and their
810 controls?, *Philos. Trans. R. Soc. B Biol. Sci.*, doi:10.1098/rstb.2013.0122, 2013.
811
- 812 Chiavegato, M. B., Powers, W. J., Carmichael, D. and Rowntree, J. E.: Pasture-derived
813 greenhouse gas emissions in cow-calf production systems, *J. Anim. Sci.*, doi:10.2527/jas.2014-
814 8134, 2015.
815
- 816 Chen, Z., Ding, W., Xu, Y., Müller, C., Yu, H. and Fan, J.: Increased N₂O emissions during
817 soil drying after waterlogging and spring thaw in a record wet year, *Soil Biol. Biochem.*,
818 doi:10.1016/j.soilbio.2016.07.016, 2016.
819
- 820 Ciais, P., Reichstein, M., Viovy, N., Granier, A., Ogée, J., Allard, V., Aubinet, M., Buchmann,
821 N., Bernhofer, C., Carrara, A., Chevallier, F., De Noblet, N., Friend, A. D., Friedlingstein, P.,
822 Grünwald, T., Heinesch, B., Kerönen, P., Knöhl, A., Krinner, G., Loustau, D., Manca, G.,
823 Matteucci, G., Miglietta, F., Ourcival, J. M., Papale, D., Pilegaard, K., Rambal, S., Seufert, G.,
824 Soussana, J. F., Sanz, M. J., Schulze, E. D., Vesala, T. and Valentini, R.: Europe-wide reduction
825 in primary productivity caused by the heat and drought in 2003, *Nature*,
826 doi:10.1038/nature03972, 2005.
827
- 828 Cowan, N. J., Levy, P. E., Famulari, D., Anderson, M., Drewer, J., Carozzi, M., Reay, D. S.
829 and Skiba, U. M.: The influence of tillage on N₂O fluxes from an intensively managed grazed
830 grassland in Scotland, *Biogeosciences*, doi:10.5194/bg-13-4811-2016, 2016.
831
- 832 Denmead, O. T.: Approaches to measuring fluxes of methane and nitrous oxide between
833 landscapes and the atmosphere, *Plant Soil*, doi:10.1007/s11104-008-9599-z, 2008.
834
- 835 Drewer, J., Anderson, M., Levy, P. E., Scholtes, B., Helfter, C., Parker, J., Rees, R. M. and
836 Skiba, U. M.: The impact of ploughing intensively managed temperate grasslands on N₂O,
837 CH₄ and CO₂ fluxes, *Plant Soil*, doi:10.1007/s11104-016-3023-x, 2017.
838
- 839 Eugster, W. and Plüss, P.: A fault-tolerant eddy covariance system for measuring CH₄ fluxes,
840 Agric. For. Meteorol., doi:10.1016/j.agrformet.2009.12.008, 2010.
841
- 842 Eugster, W. and Merbold, L.: Eddy covariance for quantifying trace gas fluxes from soils,
843 SOIL, doi:10.5194/soil-1-187-2015, 2015.
844
- 845 Felber, R., Münger, A., Neftel, A. and Ammann, C.: Eddy covariance methane flux
846 measurements over a grazed pasture: Effect of cows as moving point sources, *Biogeosciences*,
847 doi:10.5194/bg-12-3925-2015, 2015.
848
- 849 Flechard, C. R., Ambus, P., Skiba, U., Rees, R. M., Hensen, A., van Amstel, A., Dasselaar, A.
850 van den P. van, Soussana, J. F., Jones, M., Clifton-Brown, J., Raschi, A., Horvath, L., Neftel,
851 A., Jocher, M., Ammann, C., Leifeld, J., Fuhrer, J., Calanca, P., Thalman, E., Pilegaard, K., Di
852 Marco, C., Campbell, C., Nemitz, E., Hargreaves, K. J., Levy, P. E., Ball, B. C., Jones, S. K.,
853 van de Bulk, W. C. M., Groot, T., Blom, M., Domingues, R., Kasper, G., Allard, V., Ceschia,
854 E., Cellier, P., Laville, P., Henault, C., Bizouard, F., Abdalla, M., Williams, M., Baronti, S.,
855 Berretti, F. and Grosz, B.: Effects of climate and management intensity on nitrous oxide
856 emissions in grassland systems across Europe, *Agric. Ecosyst. Environ.*,
857 doi:10.1016/j.agee.2006.12.024, 2007.



- 858
859 Foken, T., Gockede, M., Mauder, M., Mahrt, L., Amiro, B. and Munger, W.: Handbook of
860 Micrometeorology: A Guide for surface flux measurement and analysis: Chapter 9: POST-
861 FIELD DATA QUALITY CONTROL., 2004.
862
863 Foken, T., Göockede, M., Mauder, M., Mahrt, L., Amiro, B. and Munger, W.: Post-Field Data
864 Quality Control, in Handbook of Micrometeorology., 2006.
865
866 Fratini, G., McDermitt, D. K. and Papale, D.: Eddy-covariance flux errors due to biases in gas
867 concentration measurements: Origins, quantification and correction, Biogeosciences,
868 doi:10.5194/bg-11-1037-2014, 2014.
869
870 Fratini, G. and Mauder, M.: Towards a consistent eddy-covariance processing: An
871 intercomparison of EddyPro and TK3, Atmos. Meas. Tech., doi:10.5194/amt-7-2273-2014,
872 2014.
873
874 Fuchs, K., Hörtnagl, L., Buchmann, N., Eugster, W., Snow, V. and Merbold, L.: Management
875 matters: Testing a mitigation strategy for nitrous oxide emissions using legumes on intensively
876 managed grassland, Biogeosciences, doi:10.5194/bg-15-5519-2018, 2018.
877
878 Fuchs, K., Merbold, L., Buchmann, N., Bretscher, D., Brilli, L., Fitton, N., Topp, C. F. E.,
879 Klumpp, K., Lieffering, M., Martin, R., Newton, P. C. D., Rees, R. M., Rolinski, S., Smith, P.
880 and Snow, V.: Multimodel Evaluation of Nitrous Oxide Emissions From an Intensively
881 Managed Grassland, J. Geophys. Res. Biogeosciences, 125(1), 1–21,
882 doi:10.1029/2019JG005261, 2020.
883
884 Dengel, S., Levy, P. E., Grace, J., Jones, S. K. and Skiba, U. M.: Methane emissions from
885 sheep pasture, measured with an open-path eddy covariance system, Glob. Chang. Biol.,
886 doi:10.1111/j.1365-2486.2011.02466.x, 2011.
887
888 Hartmann, A. A. and Niklaus, P. A.: Effects of simulated drought and nitrogen fertilizer on
889 plant productivity and nitrous oxide (N₂O) emissions of two pastures, Plant Soil,
890 doi:10.1007/s11104-012-1248-x, 2012.
891
892 Hopkins, A. and Del Prado, A.: Implications of climate change for grassland in Europe:
893 Impacts, adaptations and mitigation options: A review, Grass Forage Sci., doi:10.1111/j.1365-
894 2494.2007.00575.x, 2007.
895
896 Hörtnagl, L. and Wohlfahrt, G.: Methane and nitrous oxide exchange over a managed hay
897 meadow, Biogeosciences, doi:10.5194/bg-11-7219-2014, 2014.
898
899 Hörtnagl, L., Barthel, M., Buchmann, N., Eugster, W., Butterbach-Bahl, K., Díaz-Pinés, E.,
900 Zeeman, M., Klumpp, K., Kiese, R., Bahn, M., Hammerle, A., Lu, H., Ladreiter-Knauss, T.,
901 Burri, S. and Merbold, L.: Greenhouse gas fluxes over managed grasslands in Central Europe,
902 Glob. Chang. Biol., doi:10.1111/gcb.14079, 2018.
903
904 Imer, D., Merbold, L., Eugster, W. and Buchmann, N.: Temporal and spatial variations of soil
905 CO₂, CH₄ and N₂O fluxes at three differently managed grasslands, Biogeosciences,
906 doi:10.5194/bg-10-5931-2013, 2013.
907



- 908 Jones, S. K., Helfter, C., Anderson, M., Coyle, M., Campbell, C., Famulari, D., Di Marco, C.,
909 Van Dijk, N., Sim Tang, Y., Topp, C. F. E., Kiese, R., Kindler, R., Siemens, J., Schrumpf, M.,
910 Kaiser, K., Nemitz, E., Levy, P. E., Rees, R. M., Sutton, M. A. and Skiba, U. M.: The nitrogen,
911 carbon and greenhouse gas budget of a grazed, cut and fertilised temperate grassland,
912 Biogeosciences, doi:10.5194/bg-14-2069-2017, 2017.
913
- 914 Kim, Y. and Tanaka, N.: Fluxes of CO₂, N₂O and CH₄ by 222Rn and chamber methods in
915 cold-temperate grassland soil, northern Japan, Soil Sci. Plant Nutr.,
916 doi:10.1080/00380768.2014.967167, 2015.
917
- 918 Knox, S. H., Sturtevant, C., Matthes, J. H., Koteen, L., Verfaillie, J. and Baldocchi, D.:
919 Agricultural peatland restoration: Effects of land-use change on greenhouse gas (CO₂ and
920 CH₄) fluxes in the Sacramento-San Joaquin Delta, Glob. Chang. Biol., doi:10.1111/gcb.12745,
921 2015.
922
- 923 Krol, D. J., Jones, M. B., Williams, M., Richards, K. G., Bourdin, F. and Lanigan, G. J.: The
924 effect of renovation of long-term temperate grassland on N₂O emissions and N leaching from
925 contrasting soils, Sci. Total Environ., doi:10.1016/j.scitotenv.2016.04.052, 2016.
926
- 927 Kroon, P. S., Hensen, A., Jonker, H. J. J., Zahniser, M. S., Van't Veen, W. H. and Vermeiden,
928 A. T.: Suitability of quantum cascade laser spectroscopy for CH₄ and N₂O eddy covariance
929 flux measurements, Biogeosciences, doi:10.5194/bg-4-715-2007, 2007.
930
- 931 Kroon, P. S., Vesala, T. and Grace, J.: Flux measurements of CH₄ and N₂O exchanges, Agric.
932 For. Meteorol., doi:10.1016/j.agrformet.2009.11.017, 2010.
933
- 934 Lal, R.: Soil carbon sequestration impacts on global climate change and food security, Science
935 (80-.), doi:10.1126/science.1097396, 2004.
936
- 937 Laubach, J., Barthel, M., Fraser, A., Hunt, J. E. and Griffith, D. W. T.: Combining two
938 complementary micrometeorological methods to measure CH₄ and N₂O fluxes over pasture,
939 Biogeosciences, doi:10.5194/bg-13-1309-2016, 2016.
940
- 941 Lundegardh, H.: Carbon dioxide evolution of soil and crop growth, Soil Sci.,
942 doi:10.1097/00010694-192706000-00001, 1927.
943
- 944 MacDonald, J. D., Rochette, P., Chantigny, M. H., Angers, D. A., Royer, I. and Gasser, M. O.:
945 Ploughing a poorly drained grassland reduced N₂O emissions compared to chemical fallow,
946 Soil Tillage Res., doi:10.1016/j.still.2010.09.005, 2011.
947
- 948 MacKenzie, A. F., Fan, M. X. and Cadrian, F.: Nitrous oxide emission as affected by tillage,
949 corn-soybean-alfalfa rotations and nitrogen fertilization, in Canadian Journal of Soil Science.,
950 1997.
951
- 952 Matzner, E. and Borken, W.: Do freeze-thaw events enhance C and N losses from soils of
953 different ecosystems? A review, Eur. J. Soil Sci., doi:10.1111/j.1365-2389.2007.00992.x,
954 2008.
955



- 956 Merbold, L., Eugster, W., Stieger, J., Zahniser, M., Nelson, D. and Buchmann, N.: Greenhouse
957 gas budget (CO₂, CH₄ and N₂O) of intensively managed grassland following restoration,
958 Glob. Chang. Biol., doi:10.1111/gcb.12518, 2014.
959
960 Mishurov, M. and Kiely, G.: Gap-filling techniques for the annual sums of nitrous oxide fluxes,
961 Agric. For. Meteorol., doi:10.1016/j.agrformet.2011.07.014, 2011.
962
963 Moffat, A. M., Papale, D., Reichstein, M., Hollinger, D. Y., Richardson, A. D., Barr, A. G.,
964 Beckstein, C., Braswell, B. H., Churkina, G., Desai, A. R., Falge, E., Gove, J. H., Heimann,
965 M., Hui, D., Jarvis, A. J., Kattge, J., Noormets, A. and Stauch, V. J.: Comprehensive
966 comparison of gap-filling techniques for eddy covariance net carbon fluxes, Agric. For.
967 Meteorol., doi:10.1016/j.agrformet.2007.08.011, 2007.
968
969 Mudge, P. L., Wallace, D. F., Rutledge, S., Campbell, D. I., Schipper, L. A. and Hosking, C.
970 L.: Carbon balance of an intensively grazed temperate pasture in two climatically: Contrasting
971 years, Agric. Ecosyst. Environ., doi:10.1016/j.agee.2011.09.003, 2011.
972
973 Necpálová, M., Casey, I. and Humphreys, J.: Effect of ploughing and reseeding of permanent
974 grassland on soil N, N leaching and nitrous oxide emissions from a clay-loam soil, Nutr. Cycl.
975 Agroecosystems, doi:10.1007/s10705-013-9564-y, 2013.
976
977 Nemitz, E., Mammarella, I., Ibrom, A., Aurela, M., Burba, G. G., Dengel, S., Gielen, B., Grelle,
978 A., Heinesch, B., Herbst, M., Hörtnagl, L., Klemedtsson, L., Lindroth, A., Lohila, A.,
979 McDermitt, D. K., Meier, P., Merbold, L., Nelson, D., Nicolini, G., Nilsson, M. B., Peltola, O.,
980 Rinne, J. and Zahniser, M.: Standardisation of eddy-covariance flux measurements of methane
981 and nitrous oxide, Int. Agrophysics, doi:10.1515/intag-2017-0042, 2018.
982
983 Parkin, T. B., Venterea, R. T. and Hargreaves, S. K.: Calculating the Detection Limits of
984 Chamber-based Soil Greenhouse Gas Flux Measurements, J. Environ. Qual.,
985 doi:10.2134/jeq2011.0394, 2012.
986
987 Pavelka, M., Acosta, M., Kiese, R., Altimir, N., Brümmer, C., Crill, P., Darenova, E., Fuß, R.,
988 Gielen, B., Graf, A., Klemedtsson, L., Lohila, A., Longdoz, B., Lindroth, A., Nilsson, M.,
989 Jiménez, S. M., Merbold, L., Montagnani, L., Peichl, M., Pihlatie, M., Pumpanen, J., Ortiz, P.
990 S., Silvennoinen, H., Skiba, U., Vestin, P., Weslien, P., Janous, D. and Kutsch, W.:
991 Standardisation of chamber technique for CO₂, N₂O and CH₄ fluxes measurements from
992 terrestrial ecosystems, Int. Agrophysics, 32(4), 569–587, doi:10.1515/intag-2017-0045, 2018.
993
994 Pumpanen, J., Kolari, P., Ilvesniemi, H., Minkkinen, K., Vesala, T., Niinistö, S., Lohila, A.,
995 Larmola, T., Morero, M., Pihlatie, M., Janssens, I., Yuste, J. C., Grünzweig, J. M., Reth, S.,
996 Subke, J. A., Savage, K., Kutsch, W., Østreng, G., Ziegler, W., Anthoni, P., Lindroth, A. and
997 Hari, P.: Comparison of different chamber techniques for measuring soil CO₂ efflux, Agric.
998 For. Meteorol., doi:10.1016/j.agrformet.2003.12.001, 2004.
999
1000 Reichstein, M., Falge, E., Baldocchi, D., Papale, D., Aubinet, M., Berbigier, P., Bernhofer, C.,
1001 Buchmann, N., Gilmanov, T., Granier, A., Grünwald, T., Havráneková, K., Ilvesniemi, H.,
1002 Janous, D., Knöhl, A., Laurila, T., Lohila, A., Loustau, D., Matteucci, G., Meyers, T., Miglietta,
1003 F., Ourcival, J. M., Pumpanen, J., Rambal, S., Rotenberg, E., Sanz, M., Tenhunen, J., Seufert,
1004 G., Vaccari, F., Vesala, T., Yakir, D. and Valentini, R.: On the separation of net ecosystem



- 1005 exchange into assimilation and ecosystem respiration: Review and improved algorithm, *Glob. Chang. Biol.*, doi:10.1111/j.1365-2486.2005.001002.x, 2005.
1006
1007
1008 Rochette, P., Ellert, B., Gregorich, E. G., Desjardins, R. L., Pattey, E., Lessard, R. and Johnson,
1009 B. G.: Description of a dynamic closed chamber for measuring soil respiration and its
1010 comparison with other techniques, in *Canadian Journal of Soil Science.*, 1997.
1011
1012 Schönbach, P., Wolf, B., Dickhöfer, U., Wiesmeier, M., Chen, W., Wan, H., Gierus, M.,
1013 Butterbach-Bahl, K., Kögel-Knabner, I., Susenbeth, A., Zheng, X. and Taube, F.: Grazing
1014 effects on the greenhouse gas balance of a temperate steppe ecosystem, *Nutr. Cycl. Agroecosystems*, doi:10.1007/s10705-012-9521-1, 2012.
1015
1016
1017 Schulze, E. D., Luyssaert, S., Ciais, P., Freibauer, A., Janssens, I. A., Soussana, J. F., Smith,
1018 P., Grace, J., Levin, I., Thiruchittampalam, B., Heimann, M., Dolman, A. J., Valentini, R.,
1019 Bousquet, P., Peylin, P., Peters, W., Rödenbeck, C., Etiope, G., Vuichard, N., Wattenbach, M.,
1020 Nabuurs, G. J., Poussi, Z., Nieschulze, J. and Gash, J. H.: Importance of methane and nitrous
1021 oxide for Europe's terrestrial greenhouse-gas balance, *Nat. Geosci.*, doi:10.1038/ngeo686,
1022 2009.
1023
1024 Skiba, U., Hargreaves, K. J., Beverland, I. J., O'Neill, D. H., Fowler, D. and Moncrieff, J. B.:
1025 Measurement of field scale N₂O emission fluxes from a wheat crop using micrometeorological
1026 techniques, *Plant Soil*, doi:10.1007/BF00011300, 1996.
1027
1028 Skiba, U., Jones, S. K., Drever, J., Helfter, C., Anderson, M., Dinsmore, K., McKenzie, R.,
1029 Nemitz, E. and Sutton, M. A.: Comparison of soil greenhouse gas fluxes from extensive and
1030 intensive grazing in a temperate maritime climate, *Biogeosciences*, doi:10.5194/bg-10-1231-
1031 2013, 2013.
1032
1033 Smith, P., Martino, D., Cai, Z., Gwary, D., Janzen, H., Kumar, P., McCarl, B., Ogle, S.,
1034 O'Mara, F., Rice, C., Scholes, B., Sirotenko, O., Howden, M., McAllister, T., Pan, G.,
1035 Romanenkov, V., Schneider, U., Towprayoon, S., Wattenbach, M. and Smith, J.: Greenhouse
1036 gas mitigation in agriculture, *Philos. Trans. R. Soc. B Biol. Sci.*, doi:10.1098/rstb.2007.2184,
1037 2008.
1038
1039 Stocker, T. F., Qin, D., Plattner, G. K., Tignor, M. M. B., Allen, S. K., Boschung, J., Nauels,
1040 A., Xia, Y., Bex, V. and Midgley, P. M.: Climate change 2013 the physical science basis:
1041 Working Group I contribution to the fifth assessment report of the intergovernmental panel on
1042 climate change., 2013.
1043
1044 Teh, Y. A., Silver, W. L., Sonnentag, O., Detto, M., Kelly, M. and Baldocchi, D. D.: Large
1045 Greenhouse Gas Emissions from a Temperate Peatland Pasture, *Ecosystems*,
1046 doi:10.1007/s10021-011-9411-4, 2011.
1047
1048 Vellinga, T. V., van den Pol-van Dasselaar, A. and Kuikman, P. J.: The impact of grassland
1049 ploughing on CO₂ and N₂O emissions in the Netherlands, *Nutr. Cycl. Agroecosystems*,
1050 doi:10.1023/b:fres.0000045981.56547.db, 2004.
1051
1052 Vickers, D. and Mahrt, L.: Quality control and flux sampling problems for tower and aircraft
1053 data, *J. Atmos. Ocean. Technol.*, doi:10.1175/1520-0426, 1997.
1054



- 1055 Webb, E. K., Pearman, G. I. and Leuning, R.: Correction of flux measurements for density
1056 effects due to heat and water vapour transfer, *Q. J. R. Meteorol. Soc.*,
1057 doi:10.1002/qj.49710644707, 1980.
- 1058
- 1059 Wei, D., Ri, X., Tarchen, T., Wang, Y. and Wang, Y.: Considerable methane uptake by alpine
1060 grasslands despite the cold climate: In situ measurements on the central Tibetan Plateau, 2008-
1061 2013, *Glob. Chang. Biol.*, doi:10.1111/gcb.12690, 2015.
- 1062
- 1063 Wolf, S., Eugster, W., Ammann, C., Häni, M., Zielis, S., Hiller, R., Stieger, J., Imer, D.,
1064 Merbold, L. and Buchmann, N.: Contrasting response of grassland versus forest carbon and
1065 water fluxes to spring drought in Switzerland, *Environ. Res. Lett.*, doi:10.1088/1748-
1066 9326/8/3/035007, 2013.
- 1067
- 1068 Zeeman, M. J., Hiller, R., Gilgen, A. K., Michna, P., Plüss, P., Buchmann, N. and Eugster, W.:
1069 Management and climate impacts on net CO₂ fluxes and carbon budgets of three grasslands
1070 along an elevational gradient in Switzerland, *Agric. For. Meteorol.*,
1071 doi:10.1016/j.agrformet.2010.01.011, 2010.
- 1072
- 1073 Zenone, T., Zona, D., Gelfand, I., Gielen, B., Camino-Serrano, M. and Ceulemans, R.: CO₂
1074 uptake is offset by CH₄ and N₂O emissions in a poplar short-rotation coppice, *GCB Bioenergy*,
1075 doi:10.1111/gcbb.12269, 2016.
- 1076
- 1077 Zona, D., Janssens, I. A., Gioli, B., Jungkunst, H. F., Serrano, M. C. and Ceulemans, R.: N₂O
1078 fluxes of a bio-energy poplar plantation during a two years rotation period, *GCB Bioenergy*,
1079 doi:10.1111/gcbb.12019, 2013.
- 1080
- 1081
- 1082
- 1083
- 1084
- 1085
- 1086
- 1087
- 1088
- 1089
- 1090
- 1091
- 1092
- 1093
- 1094
- 1095
- 1096
- 1097



Table 1: Data availability of GHG fluxes measured over the five-year observation period. Values are given as all data possible, raw processed values and high quality (HQ) data, which were then used in the analysis. High quality data are data with a quality flag "0" and "1" from the Eddypro output only. Grey shaded areas represent time period where both methods (EC and static chambers) were used simultaneously to estimate FN2O.

Year	F _{CO₂}			F _{H₂O}			F _{CH₄} *			F _{N₂O} *		
	max data availability	raw fluxes	HQ fluxes (0,1)	max data availability	raw fluxes	HQ fluxes (0,1)	max data availability	raw fluxes	HQ fluxes (0,1)	max data availability	raw fluxes	HQ fluxes (0,1)
2010												
30min	17520	16064	10171	17520	13782	10117	17520 (365)	0 (44)	0 (44)	17520 (365)	0 (44)	0 (44)
%	100	91.68	58.05	100	78.65	57.74	100 (100)	0 (12.05)	0 (12.05)	100 (100)	0 (12.05)	0 (12.05)
2011												
30min	17520	14873	10002	17520	12868	9918	17520 (365)	0 (16)	0 (16)	17520 (365)	0 (16)	0 (16)
%	100	84.8	57.08	100	73.44	56.6	100 (100)	0 (4.38)	0 (4.38)	100 (100)	0 (4.38)	0 (4.38)
2012												
30min	17568	15361	10165	17568	13509	10821	17568	15523	10181	17568	15528	12859
%	100	87.43	57.85	100	76.89	61.59	100	88.35	57.95	100	88.38	73.19
2013												
30min	17520	14825	10409	17520	13425	10642	17520	17200	11310	17520 (365)	17200 (52)	11790 (52)
%	100	84.61	59.4	100	76.62	60.73	100	98.16	64.55	100 (100)	98.16 (14.24)	67.29 (14.24)
2014												
30min	17520	15719	10064	17520	13903	10252	17520	17207	11166	17520	17207	11886
%	100	89.71	57.43	100	79.35	58.51	100	98.2	63.72	100	98.2	68.4
All Years												
30min	87648	76842	50811	87648	67487	51750	87548 (730)	49930 (60)	32657 (60)	87648 (1826)	49935 (112)	36635 (112)
%	100	87.67	57.97	100	76.99	59.04	100 (100)	57.03 (8.22)	37.30 (8.22)	100 (100)	57.03 (6.13)	41.94 (6.13)

* data availability in parenthesis are based on static manual chambers (2010 and 2011), approx. biweekly measurements ($n = 16$) as well as during summer 2013 ($n = 10$)



Table 2: Annual average CO₂, CH₄ and N₂O fluxes and annual sums for the three GHGs as well as carbon and nitrogen gains/losses per gas species. GWP were calculated for a 100-year time horizon and based on the most recent numbers provided by IPCC (2013). Annual budgets were derived from either gap-filled manual chamber (MC) or eddy covariance (EC) measurements. Sign convention: positive values denote export/release, negative values import/uptake.

	2010 (MC)	2010 (EC)	2011 (MC)	2011 (EC)	2012 (MC)	2012 (EC)	2013 (MC)	2013 (EC)	2014 (MC)	2014 (EC)
Average CO ₂ flux $\mu\text{mol m}^{-2} \text{s}^{-1}$	-0.5	-0.7	1.04	-1.4	-1.98					
STDEV Average CO ₂ flux $\mu\text{mol m}^{-2} \text{s}^{-1}$	3.11	3.63	3.02	3.52	3.9					
g CO ₂ m ⁻²	-695.23	-978.16	1447.16	-2047.8	-2751.66					
g CO ₂ -C m ⁻²	-189.6	-266.77	394.68	-558.49	-750.45					
Global warming potential in g CO ₂ -eq. m ⁻²	-695.23	-978.16	1447.16	-2047.8	-2751.66					
% of the total budget	69	91.4	55.1	92.3	94					
Average CH ₄ flux $\text{nmol m}^{-2} \text{s}^{-1}$	-0.16	-0.16	1.91	3.67	3.92					
STDEV Average CH ₄ flux $\text{nmol m}^{-2} \text{s}^{-1}$	0.13	0.16	11.8	9.77	20.61					
g CH ₄ m ⁻²	-0.08	-0.08	0.96	1.85	1.97					
g CH ₄ -C m ⁻²	-0.06	-0.06	0.72	1.39	1.48					
Global warming potential in g CO ₂ -eq. m ⁻²	-2.24	-2.24	26.88	51.8	55.16					
% of the total budget	0.2	0.2	1	2.3	1.9					
Average N ₂ O flux $\mu\text{mol m}^{-2} \text{s}^{-1}$	0.84	0.25	3.13	0.28	0.32	0.32				
STDEV Average N ₂ O flux $\mu\text{mol m}^{-2} \text{s}^{-1}$	0.84	0.2	4.35	0.6	0.73	0.68				
g N ₂ O m ⁻²	1.17	0.34	4.36	0.39	0.45	0.45				
g N ₂ O-N m ⁻²	0.74	0.22	2.77	0.25	0.28	0.28				
Global warming potential in g CO ₂ -eq. m ⁻²	310.05	90.1	1155.4	103.35	119.25	119.25				
% of the total budget	30.8	8.4	43.9	5.4	4.1					
Total GWP potential	-387.42	-890.3	2629.44	-1892.65	-1876.75	-2577.25				

1101

1102

1103



Table 3: Average GHG flux rates per season: winter (DJF), spring (MAM), summer (JJA) and fall (SON). Values are based on gap-filled data to avoid bias from missing nighttime data (predominantly relevant for CO₂). Data are only presented when continuous measurements (eddy covariance data) were available. Sign convention: positive values denote export/release, negative

	CO ₂ ($\mu\text{mol m}^{-2} \text{s}^{-1}$)			CH ₄ ($\text{nmol m}^{-2} \text{s}^{-1}$)			N ₂ O ($\text{nmol m}^{-2} \text{s}^{-1}$)					
	DJF	MAM	JJA	SON	DJF	MAM	JJA	SON	DJF	MAM	JJA	SON
2010	0.56	-1.75	-0.79	0.01								
SD	5.39	12.07	11.34	9.31								
2011	0.48	-4.29	0.39	0.66								
SD	5.47	10.54	12.52	8.97								
2012	0.98	3.64	-0.53	-0.13	2.2	1.38	2.76	1.32	3.1	5.61	3.06	0.73
SD	5.69	9.1	13.65	8.03	14.91	11.85	10	9.94	4.77	5.52	3.19	0.92
2013	-0.2	-4.49	-1.3	0.13	2.18	5.3	3.79	3.4	0.12	0.19	0.73	0.26
SD	5.04	12.98	12.14	9.81	11.31	9.25	9.08	9.21	0.23	0.37	1.27	0.38
2014	-0.42	-5.07	-2.43	0.04	6.71	5.49	0.08	3.47	0.18	0.4	0.45	0.27
SD	6.56	12.93	12.98	9.45	22.93	31.37	8.5	1021	0.27	0.78	0.87	0.63
2010-2014	0.28	-2.39	-0.89	0.14	3.69	4.06	2.21	2.73	1.14	2.07	1.42	0.42
SD	5.68	12.06	12.58	9.14	17.15	20.11	9.31	9.81	3.09	4.08	2.35	0.71

1104

1105

1106



Table 4: Carbon and partial nitrogen budgets (excluding NH₃, NO_x and N₂ emissions as well as N deposition is not included) for the Chamau (CH-Cha) site in 2010–2014. Values are given in kg ha⁻¹. Inputs/gains are indicated with “-” and losses/exports are indicated with “+”. While management information was available for both parcels (A and B), flux measurements are an integrate of both parcels.

	2010	2011	2012	2013	2014	Total 2010 - 2014		
	Carbon	Nitrogen	Carbon	Nitrogen	Carbon	Nitrogen	Carbon	Nitrogen
Fertilizer (kg ha ⁻¹) - Parcel A	-1425.53	-253.09	-1222.06	-253.97	-2242.51	-271.12	-926.81	-213.19
Fertilizer (kg ha ⁻¹) - Parcel A	-1487.1	-194.3	-1509.9	-258.3	-2229	-293.2	-1001.1	-240
Harvest (kg ha ⁻¹) - Parcel B	3449.26	221.85	2570.3	165.32	1684.88	108.37	4393.9	282.61
Harvest (kg ha ⁻¹) - Parcel B	2018.6	129.8	1952.2	125.6	1481.2	95.3	4174.8	268.5
Flux (CO ₂ -C kg ha ⁻¹)	-1896.6		-2667.7		3946.8		-5584.9	
Flux (CH ₄ -C kg ha ⁻¹)	-0.6		-0.6		7.2		13.9	
Flux (N ₂ O-N kg ha ⁻¹)		7.4		2.2		27.7		2.8
Total Budget - Parcel A	126.53	-23.84	-1320.06	-86.45	3396.37	-135.05	-2103.91	72.22
Total Budget - Parcel B	-1365.7	-57.1	-2226	-130.5	3206.2	-170.2	-2397.3	31.3
							-1813.1	248.8
							-4595.9	-77.7

1107

1108

1109



Table 5: Existing studies investigating the GHG exchange over pastures following ploughing. Results presented show the flux magnitude following ploughing and are rounded values of the individual presented in the papers. Values were converted to similar units (mg CO₂-C m⁻² h⁻¹ and µg CH₄-C m⁻² h⁻¹ and µg N₂O-N m⁻² h⁻¹). Based on Web of Knowledge search July 15th 2017 with the search terms "grassland", "pasture", "greenhouse gas", "ploughing" and/or "tillage". Only two studies representing conversion from pasture to cropland or other systems were included in this table.

Publication	Grassland type	Observation Period	Measurement technique	Supporting Information		
				CO ₂ -C	CH ₄ -C	N ₂ O-N
Bertora et al. 2007	permanent pasture	62 days approx five years	Incubation study of soil cores	188 - 330 mg kg ⁻¹ soil *	NA	50 - 1000 µg kg ⁻¹ soil !
Li et al. 2015	managed grassland	three years of cropping	static GHG chamber	> 600 mg m ⁻² h ⁻¹ &	NA	> 1000 µg m ⁻² h ⁻¹ &
Buchen et al. 2016	managed grassland	44 days	¹⁵ N isotopic measurements	NA	100 - 1000 µg m ⁻² h ⁻¹	
Krol et al. 2016	permanent grassland	17 weeks	static GHG chambers on lysimeter	NA	NA	3000 µg m ⁻² h ⁻¹ %
Cowan et al. 2016	permanent grassland	175 days	eddy covariance	NA	500 - 700 µg m ⁻² h ⁻¹ !	
Drewer et al. 2016	permanent grassland poorly drained	three years	static GHG chambers/eddy covariance	250 - 2000 mg m ⁻² h ⁻¹	1000 - 8000 µg m ⁻² h ⁻¹	500 - 7000 µg m ⁻² h ⁻¹ §
MacDonald et al. 2011	grassland		static GHG chambers	NA	NA	> 6000 µg m ⁻² h ⁻¹ !
Estravillo et al. 2001	permanent pasture		incubation study of soil cores	NA	NA	1800 - 5000 µg m ⁻² h ⁻¹ !
Merbold et al. 2014	permanent grassland	five years	static GHG chambers/eddy covariance	> 400 mg m ⁻² h ⁻¹ #	non-different from zero	> 2000 µg m ⁻² h ⁻¹ #
and this study	permanent grassland	five years				

* cumulative fluxes over 62 days, & conversion from grassland to cropland, ! approximate value recalculated from figure in the paper, % approximate peak emission following restoration calculated from figure in the paper, § approximate value recalculated from figures presented in both paper, # approximate value recalculated from figure in the paper, § approximate value presented in Figure 3 in the publication, # peak emissions

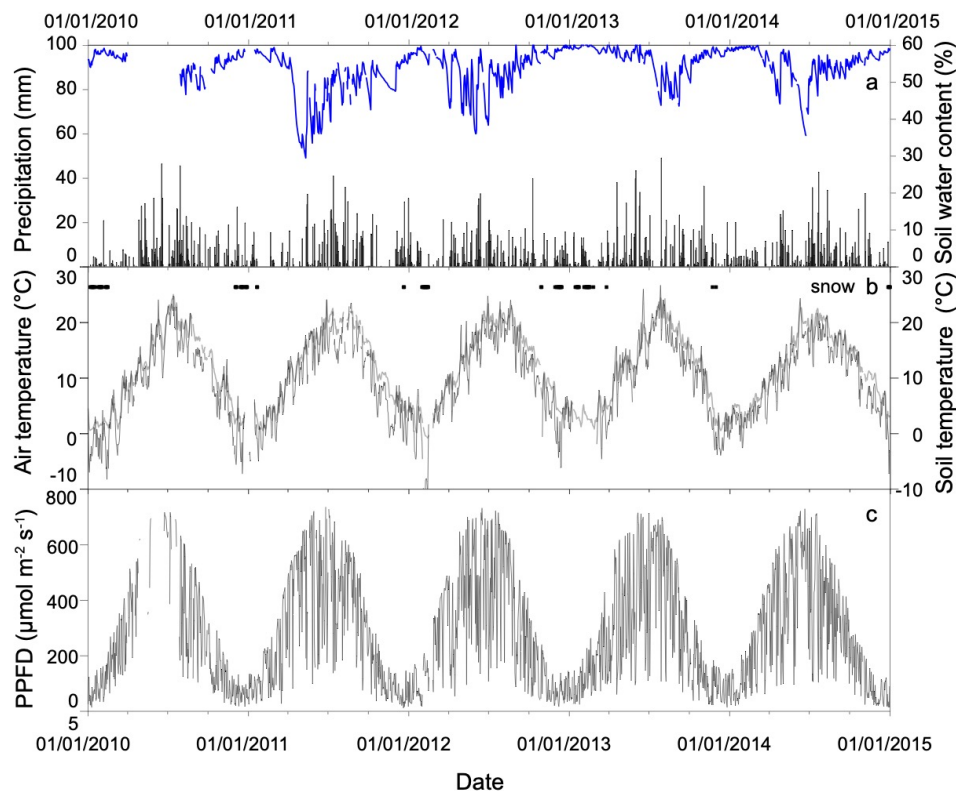


Figure 1: Weather conditions during the years 2010 – 2014. Weather data were measured with our meteorological sensors installed on site. (a) Daily sum of precipitation (mm) and soil water content (blue line, %) measured at 5 cm soil depth; (b) daily averaged air temperature (black line, °C), daily averaged soil temperature (grey line, °C), and days with snow cover (horizontal bars); (c) daily averaged photosynthetic photon flux density (PPFD, $\mu\text{mol m}^{-2} \text{s}^{-1}$). Snow covered days were identified with albedo calculations. Days with albedo values > 0.45 were identified as days with either snow or hoarfrost cover.

1113
1114
1115

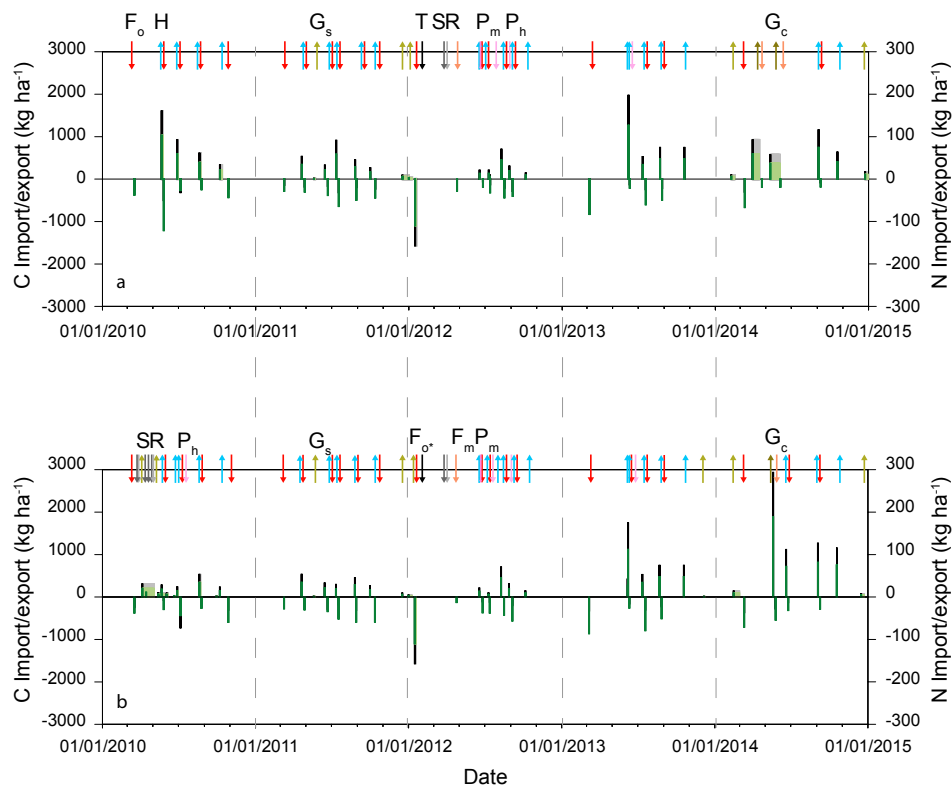


Figure 2: Management activities for both parcels (A and B in panels (a) and (b), respectively) on the CH-Cha site. Overall management varied particularly in 2010 between both parcels, whereas similar management took place between 2011 and 2014. Arrow direction indicates whether carbon (C in kg ha^{-1}) and/or nitrogen (N in kg ha^{-1}) were amended to, or exported from the site (" F_o " and " F_o^* " - organic fertilizers, slurry/manure (red); " F_m " - mineral fertilizer (light orange); "H" - harvest (light blue); " G_s " and " G_c " - grazing with sheep/cows (light/dark brown). Other coloured arrows visualize any other management activities such as pesticide application (" P_h " - herbicide (light pink); " P_m " - molluscicide (dark pink); "T" - tillage (black), "R" - rolling (light grey) and "S" - sowing (dark grey) which occurred predominantly in 2010 (parcel B) and 2012 (parcels A and B). Carbon imports and exports are indicated by black and grey bars. Thereby black indicated the start of the specific management activities and grey the duration (e.g. during grazing, " G_s "). Green colors indicate nitrogen amendments or losses, with dark green visualizing the start of the activity and light green colors indicating the duration. Sign convention: positive values denote export/release, negative values import/uptake.

1116

1117

1118

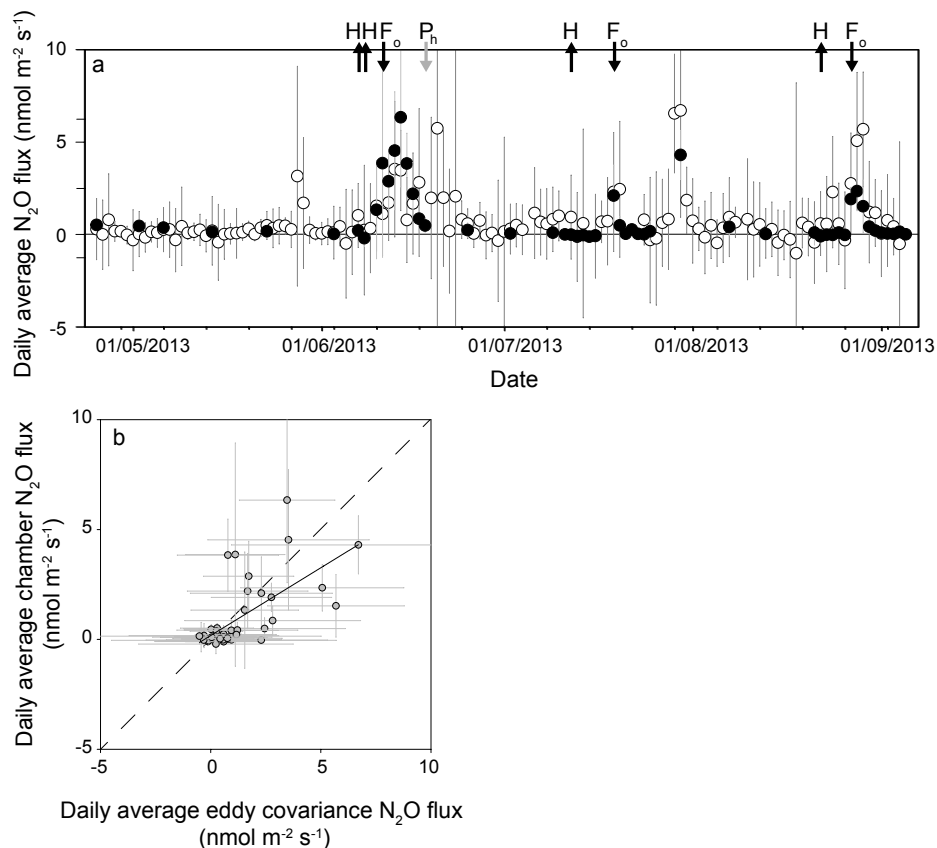


Figure 3: (a) Temporal dynamics of daily average N_2O fluxes measured with the eddy covariance (white circles) and manual greenhouse gas chambers (black circles) in 2013. Black arrows indicate management events, grey lines indicate standard deviation ("H"= harvest, " F_o " = organic fertilizer application (slurry), " P_h "= pesticide (herbicide) application);
 (b) 1:1 comparison between chamber based and eddy covariance based N_2O fluxes in 2013. The dashed line represents the 1:1 line. (Regression: $y = 0.61x + 0.17$, $r^2 = 0.4$). Sign convention: positive values denote export/release, negative values import/uptake.

1119
 1120
 1121

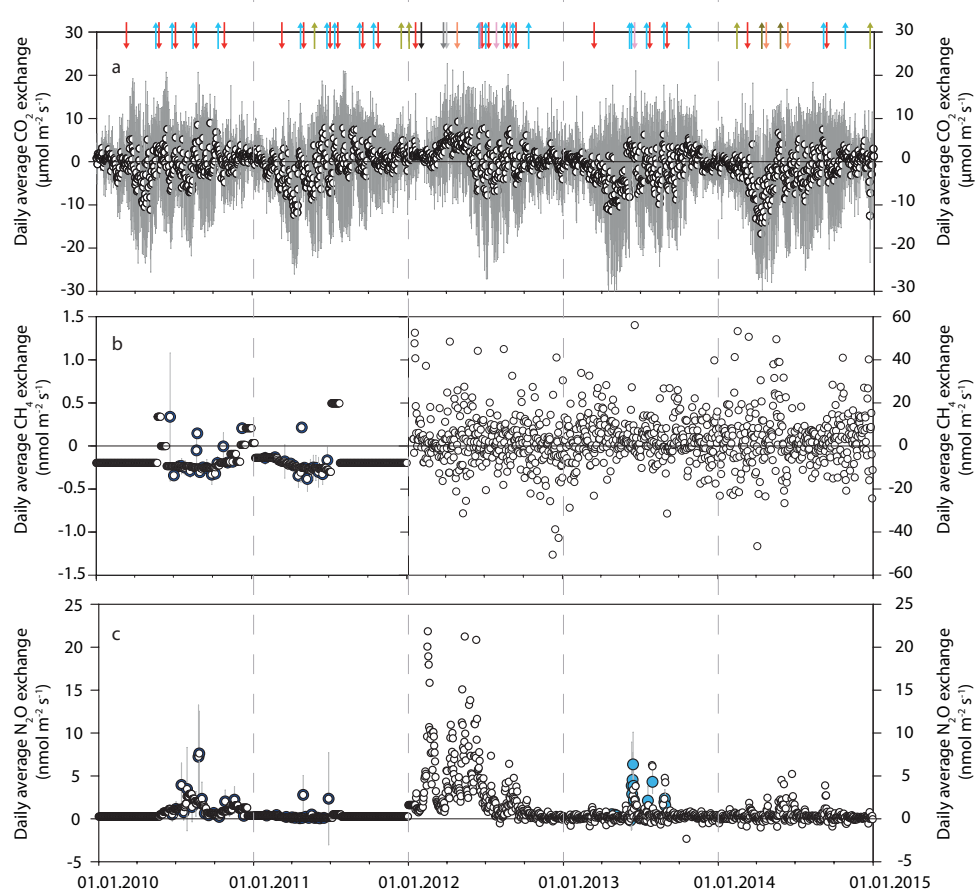


Figure 4: Temporal dynamics of gap-filled daily averaged greenhouse gas (GHG) fluxes (white circles):
 a) (CO_2 exchange in $\mu\text{mol m}^{-2} \text{s}^{-1}$); (b) CH_4 exchange in $\text{nmol m}^{-2} \text{s}^{-1}$ and (c) N_2O exchange in $\text{nmol m}^{-2} \text{s}^{-1}$. Coloured circles indicate manual chamber measurements. While both GHGs, CH_4 and N_2O were measured in 2010 and 2011 (blue circles), N_2O only was measured in 2013 (light blue circles). The grey dashed lines indicate the beginning of a new year. Same color coding as used in Figure 3 a was used to highlight management activities. Sign convention: positive values denote export/release, negative values import/uptake. Grey lines behind the circles indicate standard deviation.